

A *Ralstonia* effector RipAU impairs peanut AhSBT1.7 immunity for pathogenicity via AhPME-mediated cell wall degradation

Kun Chen^{1,2,†}, Yuhui Zhuang^{1,3,†}, Hua Chen^{1,2}, Taijie Lei^{1,2}, Mengke Li^{1,2}, Shanshan Wang^{1,2}, Lihui Wang^{1,2}, Huiwen Fu^{1,2}, Wenzhi Lu^{1,2}, Abhishek Bohra⁴, Qiaoqiao Lai^{1,2}, Xiaolin Xu^{1,2}, Vanika Garg⁵, Rutwik Barmukh⁵, Biaojun Ji^{1,2}, Chong Zhang^{1,2}, Manish K. Pandey⁶, Ronghua Tang⁷, Rajeev K. Varshney^{1,5,*}  and Weijian Zhuang^{1,2,*} 

¹Center for Legume Plant Genetics and Systems Biology, Oil Crops Research Institute, Fujian Agriculture and Forestry University, Fuzhou 350002, China,

²State Key Laboratory of Ecological Pest Control for Fujian and Taiwan Crops, College of Agriculture, Fujian Agriculture and Forestry University, Fuzhou 350002, China,

³College of Life Science, Fujian Agriculture and Forestry University, Fuzhou 350002, China,

⁴ICAR-Indian Institute of Pulses Research (IIPR), Kanpur 208024, India,

⁵Centre for Crop and Food Innovation, State Agricultural Biotechnology Centre, Food Futures Institute, Murdoch University, Murdoch 6150, Australia,

⁶International Crops Research Institute for the Semi-Arid Tropics, Hyderabad 502324, Telangana, India, and

⁷Guangxi Academy of Agriculture Science, Nanning 530007, China

Received 18 April 2024; revised 17 November 2024; accepted 23 November 2024.

*For correspondence (e-mail weijianz@fafu.edu.cn and rajeev.varshney@murdoch.edu.au).

†These authors contributed equally to this work.

SUMMARY

Bacterial wilt caused by *Ralstonia solanacearum* is a devastating disease affecting a great many crops including peanut. The pathogen damages plants via secreting type III effector proteins (T3Es) into hosts for pathogenicity. Here, we characterized RipAU was among the most toxic effectors as Δ RipAU completely lost its pathogenicity to peanuts. A serine residue of RipAU is the critical site for cell death. The RipAU targeted a subtilisin-like protease (AhSBT1.7) in peanut and both protein moved into nucleus. Heterotic expression of AhSBT1.7 in transgenic tobacco and *Arabidopsis thaliana* significantly improved the resistance to *R. solanacearum*. The enhanced resistance was linked with the upregulating ERF1 defense marker genes and decreasing pectin methylesterase (PME) activity like PME2&4 in cell wall pathways. The RipAU played toxic effect by repressing R-gene, defense hormone signaling, and AhSBTs metabolic pathways but increasing PMEs expressions. Furthermore, we discovered AhSBT1.7 interacted with AhPME4 and was colocalized at nucleus. The AhPME speeded plants susceptibility to pathogen via mediated cell wall degradation, which inhibited by AhSBT1.7 but upregulated by RipAU. Collectively, RipAU impaired AhSBT1.7 defense for pathogenicity by using PME-mediated cell wall degradation. This study reveals the mechanism of RipAU pathogenicity and AhSBT1.7 resistance, highlighting peanut immunity to bacterial wilt for future improvement.

Keywords: *Ralstonia solanacearum*, pathogenicity, RipAU, peanut, AhSBT1.7, AhPME4.

INTRODUCTION

Bacterial wilt caused by *Ralstonia solanacearum* is a damaging plant disease that reduces peanut yield by 10–30% or 100% in severe cases (Luo et al., 2019). *R. solanacearum* infection blocks the vascular tissue of plants, wilting the plant, and leading to death within a few weeks.

The pathogen has a broad host range, infecting over 50 genera and 450 species (Zhang et al., 2017). Moreover, *R. solanacearum* has a tenacious vitality and stable

pathogenicity with many effectors, making it one of the most serious plant diseases (Chen et al., 2021). The pathogenicity of *R. solanacearum* is complex, involving T3Es, the major virulence factors secreted by syringe-like type III secretion system (T3SS) into plant cells (Tan et al., 2019). The T3SS has over 20 Hrp gene clusters (Lohou et al., 2014), which regulate T3Es secretion. However, T3SS mutants of *R. solanacearum* completely lose their pathogenicity on tobacco plants, including leaf necrotic lesions

(Liuti et al., 2014). Thus, T3Es are indispensable in the pathogenicity of *R. solanacearum*.

Plants evolved two resistance strategies through long-term coevolution: Pathogen-associated molecular pattern (PAMP)-triggered immunity (PTI) and effector-triggered immune (ETI) against pathogens. PAMPs activate host plant immunity through a resistance strategy called PTI (Ausubel, 2005). Pathogens coevolved virulence proteins called effectors, to inhibit the PTI-triggered immune response (Nakano & Mukaihara, 2018). In turn, host plants further evolved the ETI, a resistance response involving effector proteins called avirulence proteins. Resistance (R) genes recognize these effector proteins, trigger cell death, and limit pathogen spread in the host (Jones & Dangl, 2006). The T3Es have few avirulence and many virulence proteins.

Thus far some virulence proteins have been identified to impair plants defenses. For example, RipAY was reported to reduce intracellular glutathione in *Arabidopsis thaliana* and conduce bacterial wilt infection (Fujiwara et al., 2016). RipAW and RipAR inhibited reactive oxygen species and the defense genes expression in *Nicotiana benthamiana* (Nakano et al., 2017). RipAL decreased salicylic acid (SA) in pepper (Nakano & Mukaihara, 2018), and RipAB inhibited the Ca²⁺ signaling in potato plants, thus, encouraging the infection (Zheng et al., 2019). RipN acted as a Nudex hydrolase, altering the NADH/NAD⁺ ratio in *A. thaliana* and inhibiting PTI (Sun et al., 2019). Effector proteins can also create conducive environment for bacteria to propagate in plants as RipI interacts with plant glutamate decarboxylases and catalyzes the biosynthesis of gamma-aminobutyric acid as a nutrient for bacteria propagation (Xian et al., 2020). Therefore, understanding the interactions between effectors and host factors is key to discovering resistance mechanisms and developing strategies for alleviating bacterial wilt disease. Unfortunately, no virulence protein was identified in peanut.

Proteolysis is important for plant development, defense, stress response, and other life processes, catalyzed by proteolytic enzymes. Serine proteolytic enzymes account for nearly 30% of proteases and are currently classified into three main classes: subtilisin-like proteases (subtilases), caseinolytic protease (CLP proteases), and kexin-type proteases (Fajing et al., 2018). Subtilases are pivotal in plant-microbe interactions, regulating plant immune responses and enhancing host resistance to pathogens (Figueiredo et al., 2014). For instance, *ATSBT1.3* triggered innate immune responses in *A. thaliana*, significantly enhancing its resistance to *Pseudomonas syringae* (Ramirez et al., 2013). The *A. thaliana* *AtSBT5.2* may transcriptionally regulate defense responses, affecting plant resistance to pathogens (Serrano et al., 2016). In tomatoes, viroids induced the expression of two subtilases, P69B and P69c. Subtilase p69 hydrolyzed specific

proteins in tomato infected by *P. syringae* (Jordá et al., 1999; Tornero et al., 1997). In cotton, jasmonic acid (JA) and ethylene (ET) induced *GBSBT1*, triggering the immune response of cotton and enhancing the resistance against *Fusarium oxysporum* and *Verticillium dahliae* infection (Duan et al., 2016). However, there is no report about the resistance mechanism of subtilases and their involvement in plant resistance to bacterial wilt.

So far, only a few effectors function in *R. solanacearum* were characterized, which still limits uncovering the complicated pathogenicity and the host resistance mechanism needed for applications. For better characterization of peanut immune reaction to *R. solanacearum*, we knocked out the whole T3Es in a peanut bacterium Rs-P.36220 based on the genome studies (Chen et al., 2021) and characterize the peanut immune reaction to *R. solanacearum* infection. We focused on effector RipAU pathogenicity and revealed its structure changes related to cell death, screened and verified its interacting proteins, and identified the pivot target *AhSBT1.7* in RipAU virulence. We characterized the function of *AhSBT1.7* who showed the high resistance in transgenic tobacco and *A. thaliana* against *R. solanacearum*. The study also revealed the mechanism underling the *AhSBT1.7*-mediated defense signaling pathway. Additionally, the study showed that *AhSBT1.7* interacted with PME *AhPME4* and inhibited its activity which positively regulates RipAU pathogenicity downstream of the *AhSBT1.7*.

RESULTS

RipAU plays a key role in *R. solanacearum* pathogenesis

Numerous *R. solanacearum* T3Es are key for their pathogenicity, wide host range, and environmental adaptability (Cong et al., 2022). *R. solanacearum* T3SS secrete T3Es proteins which interfere with the immune function of the host (Moon et al., 2021). Studies have shown that single knockouts of some T3Es, such as RipV2 (Cheng et al., 2021), RipG7 (Angot et al., 2006), RipI (Xian et al., 2020), RipAK (Wang et al., 2021), and RipAB (Zheng et al., 2019), reduce the pathogenicity of *R. solanacearum* on the host. We inoculated the peanut susceptible variety Xinhuixiaoli (XHXL) with individual single T3Es mutants of the whole mutant library and observed their phenotypes after 9 days of inoculation to clarify the pathogenicity of T3Es mutants on peanut. By phenotypes evaluation and RNA expression verification, the effector RipAU was screened (Figure 1a–e).

We verified the expression of *RipAU* mutant at the transcriptional level. The transcriptional expression of *RipAU* in wild type (WT) and the complemented *RipAU* (*CRipAU*) were similar, but the *RipAU* was not expressed in Δ *RipAU* (Figure 1a), indicating that we successfully knocked out *RipAU* and obtained the *CRipAU*. We characterized their pathogenicity comparatively. *R. solanacearum*

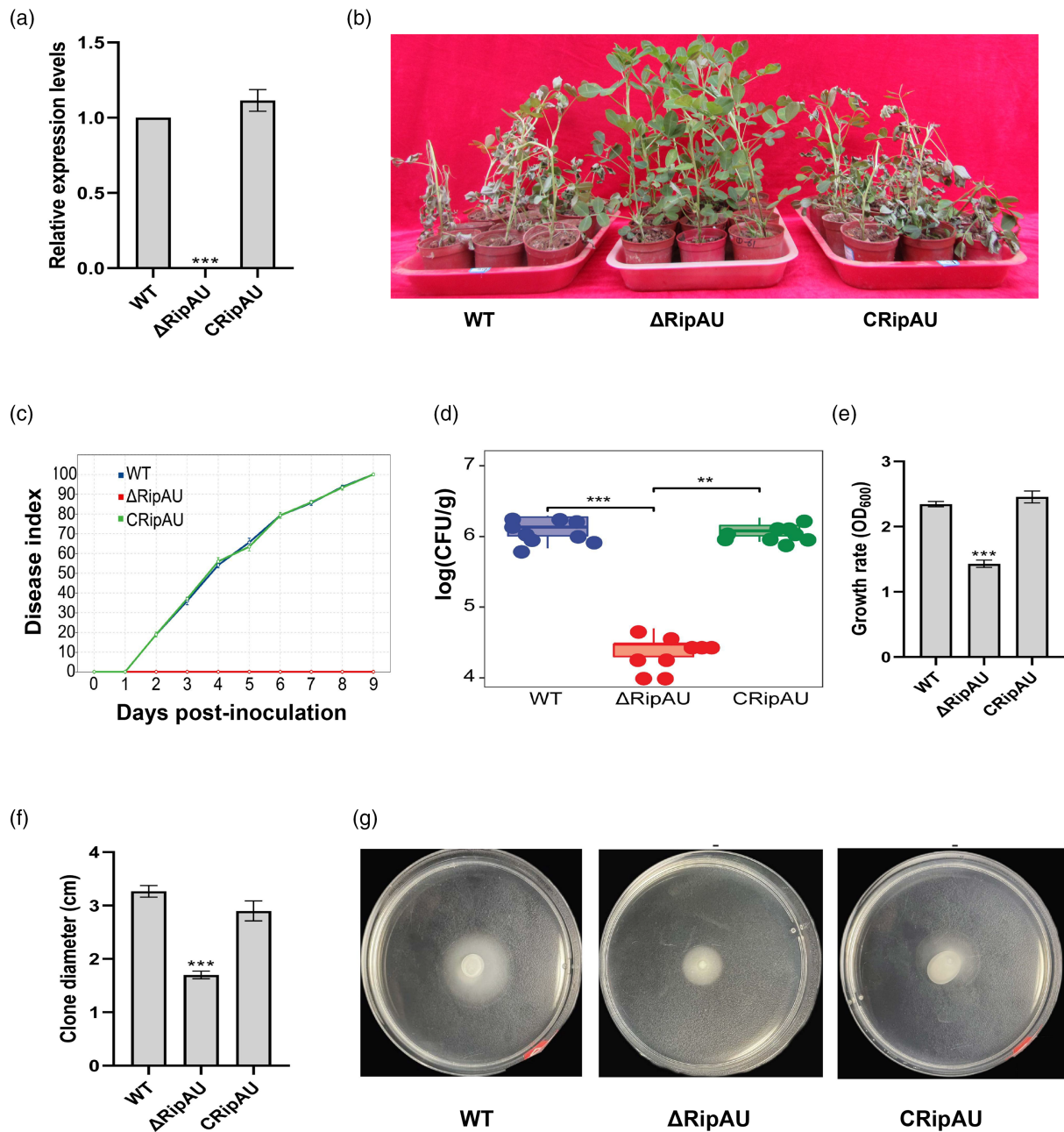


Figure 1. Functional identification of RipAU.

(a) The relative expression of RipAU in different strains with no *RipAU* transcript in Δ RipAU. The expression levels of RipAU in different strains were calculated by qRT-PCR, and three biological replicates were set up in the experiment ($n = 3$, t -test, $**P < 0.01$; $***P < 0.001$).

(b) Phenotype of WT, Δ RipAU, and CRipAU on peanut leaves at 9 DPI. Peanut XHXL was inoculated using the leaf cutting method. Observations and photos were taken on the ninth day after inoculation, and three biological replicates were set ($n = 9$).

(c) The *Ralstonia solanacearum* disease index on inoculated peanuts. Values are means \pm SE of three replicates ($n = 9$).

(d) *R. solanacearum* colonization of peanut stems. Three days after the peanuts were inoculated with *R. solanacearum*, 1 g of peanut stems were cut with sterile scissors, added with sterile water and ground, and the bacterial content was calculated by gradient dilution method.

(e) The growth rate (OD₆₀₀ value) of *R. solanacearum* after culturing on BG media for 48 h, Δ RipAU mutant shows low growth rate ($n = 3$).

(f) *R. solanacearum* colony diameter on semi-solid media, Δ RipAU has smaller clone. 5 μ l of *R. solanacearum* was cultured on semi-solid medium for 3 days and then the colony size was counted ($n = 3$).

(g) The growth morphology of *R. solanacearum*. *R. solanacearum* was cultured on semi-solid medium and photographed after 3 days of cultivation.

completely lost its pathogenicity after *RipAU* deletion, significantly reducing its reproductive ability on peanut plants than the WT and the CRipAU strains (Figure 1b–d). The

disease index of the mutant maintained zero but WT and the CRipAU strains reached 100% at 9 day post inoculation. In addition, Knocking out *RipAU* decreased the

growth rate and motility of *R. solanacearum* but still is growing (Figure 1e–g). Therefore, RipAU is a key virulence factor affecting both the pathogenicity on peanut and the motility and growth of itself.

RipAU triggers cell death and coevolves with *R. solanacearum* phylotypes

In plants, cell death of infected cells and adjacent tissues is a resistant response to pathogen attack by plant-intrinsic genetic control (Long et al., 2009). We constructed plant over-expression vectors for RipAU and transiently expressed it on tobacco leaves. After 36 h of transient expression, RipAU produced a strong necrotic causing cell death in tobacco leaves (Figure 2a,b). The necrotic sites were stained blue using trypanblue (TB) and brown using 3,3-diaminobenzidine tetra-hydrochloride (DAB) (Figure 2c). The results showed that RipAU can induce plant cell death and reactive oxygen species (H_2O_2) accumulation.

It had been shown that RipAU in GMI1000 did not induce cell death on tobacco leaves (Niu et al., 2021), which was also confirmed in our study (Figure 2a), indicating a RipAU sequence diversity in the two strains. We compared the amino acid sequences of RipAUs between Rs-P.362200 and GMI1000 and revealed six amino acid (aa) residues changes, including Q27P, M45L, S168L, H222Y, K224E, and A225P (Figure 2d). To know the residues responsible for cell death, we mutated these aa of RipAU from strain Rs-P.362200 separately and obtained three *ripAU* mutants (SL: S168L, M2: Q27P, M45L, and M3: H222Y, K224E, A225P), respectively, by site-specific mutation and performed transient expressions of them (Figure 2e). Interestingly, we found that RipAU (Rs-P.362200) lost cell death only after the S168L site mutation (Figure 2g). Since S168 of RipAU is the key amino acid site for inducing cell death response, will the mutation of this site affect the pathogenicity of *R. solanacearum*? After created CRipAU_{S168L} complementing strain, we performed

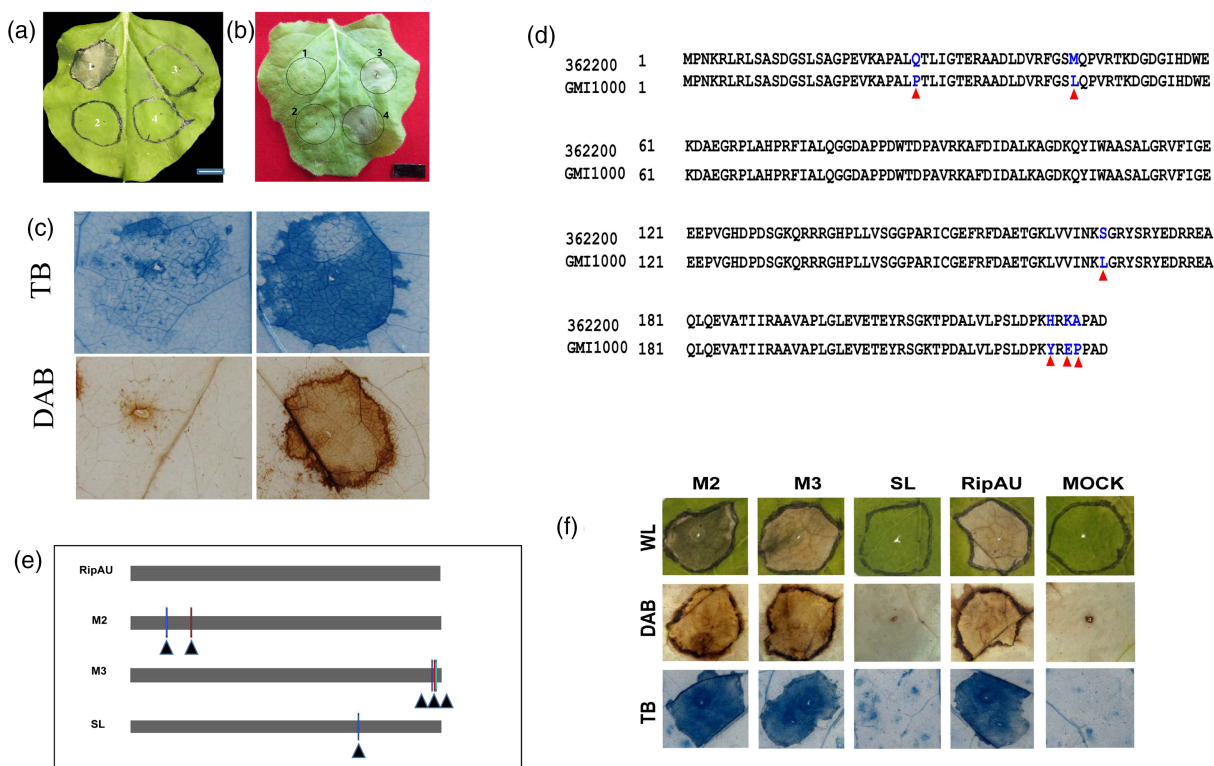


Figure 2. The cell death induced by RipAU.

(a–c) Transient expression of RipAU causes *Nicotiana benthamiana* leaf cell death. (a) The leaf in the figure was injected with: 1-RipAU from *Ralstonia solanacearum* Rs-P.362200, 2-the empty vector, 3-RipAU from GMI1000, 4-MES buffer as mock. (b, c) Trypan blue and 3,3-diaminobenzidine (DAB) staining of transiently overexpressed in tobacco leaves. 1: MES buffer, 2: empty vector, 3–4: RipAU from Rs-P.362200. Bar: 1 cm.

(d) Amino acid sequences diversity of RipAU between isolates Rs-P.362200 and GMI1000.

(e) The different sites of RipAU mutants are shown graphically. M2 represents the amino acid residues of Q27P and M45L mutants in the RipAU of P.362200. M3 represents amino acid residues of H222Y, K224E, and A225P mutants. SL represents amino acid residues of mutant S168L. Triangles mark the positions of corresponding amino acid residues.

(f) Cell death of RipAU mutants on *N. benthamiana* photographed on the third day after injection. Trypan blue and 3,3-diaminobenzidine (DAB) were used to stain the transient overexpression tobacco leaves, respectively.

evaluation in peanut together with CRipAU (Figure S1). We founded that the CRipAU (S168L) strain can restore virulence after complementing the mutant strain Δ RipAU, indicating that the mutation of S168L site did not change its pathogenicity though it lost induction of cell death. Therefore, RipAU induces cell death in tobacco, and the serine site is indispensable.

The RipAU is a protein with 228 amino acids. To clarify the distribution and evolutionary characteristics of RipAU in different phylotypes of *R. solanacearum*, the orthologous genes of RipAU were found in 89 strains with similarity >60% from NCBI and T3Es databases. Phylogenetic analysis was performed to show the orthologous genes diversity of RipAUs. The RipAUs can be clustered into five groups, which consist of *R. solanacearum* phylotypes I, IIA, IIB and IV, and type IIA have separated into IIA1 and IIA2 subgroups (Figure S2). The RipAU in strain Rs-P.362200 is clustered with RipAUs in phylotype I strain (Figure S2), indicating RsRipAU coevolves with the phylotypes diversity of *R. solanacearum* pathogen.

RipAU interacts with subtilisin-like protease SBT1.7 in peanut

We performed Y2H screening of a peanut cDNA library and obtained the RipAU target genes in peanut which we used to investigate its pathogenesis (Table S1). An AhSBT1.7 containing 755 aa with three functional domains (I9, S8, and PA) was screened (Figure 3a). Y2H results showed a strong interaction between AhSBT1.7 and RipAU (Figure 3b), and BiFC tests confirmed that interaction (Figure 3c). Transient individual expressions of GFP::RipAU and GFP::AhSBT1.7 in *N. benthamiana* demonstrated that RipAU localizes to the cytoplasm and nucleus, and AhSBT1.7 remains at the cytoplasmic areas (Figure S3). Interestingly, the co-transformed RipAU and AhSBT1.7 in *N. benthamiana* leaves were co-localized in the nucleus in the BiFC assay (Figure 3c). Therefore, the RipAU-AhSBT1.7 interaction may be important for the transcriptional changes for its pathogenicity.

Truncating the three functional domains of AhSBT1.7 through Y2H and BiFC evaluations showed that RipAU interacted with the AhSBT1.7 S8 domain but not with the other two domains (Figure 3b,c). Although the serine site of RipAU affects its cell death, Y2H and BiFC experiments showed that RipAU_{S168L} interacted with AhSBT1.7 (Figure 3b,c).

Transgenic AhSBT1.7 significantly increased plant resistance to *R. solanacearum*

Several plant stress defenses involve SBT1.7, but the SBT1.7 function in bacterial wilt is unknown. We transformed AhSBT1.7 into a high susceptible tobacco cultivar Honghuadajinyuan (HD) and obtained stable genetic lines. We also transformed *A. thaliana* and obtained three stable

lines and the NbSBT1.7 gene into HD to determine whether NbSBT1.7 regulates host resistance to bacterial wilt. Inoculating transgenic tobacco lines with *R. solanacearum* showed that AhSBT1.7 overexpression significantly improves the resistance of transgenic plants to *R. solanacearum* compared to the non-transgenic control (HD) and the highly resistant control tobacco Yanyan 97 (YY97) plants with much less bacterial wilt and death rate (Figure 4a). We investigated the bacterial colonization among SBT1.7 overexpression lines in comparison with nontransgenic HD and YY97. Transgenic lines significantly inhibited bacterial colonization, which was stronger than that of YY97, and the plants had a much lower disease index (Figure 4b,c). Dissecting the stems of *R. solanacearum*-inoculated tobacco after 14 days revealed that the interior of HD stems was rotten and black, while the stems of transgenic tobacco had no significant changes (Figure S4). Moreover, *R. solanacearum* inoculation turned the roots of HD brown, but no necrosis was observed in the roots of transgenic tobacco (Figure S4). Transgenic *A. thaliana* with AhSBT1.7 (Figure S5) and transgenic tobacco with NbSBT1.7 (Figure S6) showed similar results. In general, the disease index of nontransgenic tobacco reached 100%, and that of transgenic tobacco was approximately 50% (Figure 4). However, transgenic *A. thaliana* was more resistant to bacterial wilt after *R. solanacearum* inoculation with the disease index approximately 30% (Figure S5). All these results indicate that the virulent RipAU-targeted SBT1.7 is a disease-resistance gene. This imply that AhSBT1.7 may be involved in the host immune response during the peanut and *R. solanacearum* interaction.

AhSBT1.7 improves plant defense by downregulating PME

The previous results showed that AhSBT1.7 is a disease-resistance gene, but the signaling pathways it uses to regulate plant resistance were unknown. Thus, we evaluated the resistance marker genes in signaling pathways, like NPR1 and ICS1 in salicylic acid (SA) signaling, JAZ1, JAR1 and PDF1.2 in methyl jasmonate (JA), ERF1 and ACS6 in ethylene (ET), RAR1 in pattern-triggered immunity (PTI), NDR1 and EDS1 in effector-triggered immunity (ETI) and PME4 and PME2 in PMEs cell wall signaling pathways were investigated, by qRT-PCR (Figure S7). It seemed that AhSBT1.7 could not upregulate, or even inhibit the transcriptional levels of most signaling (like SA, JA, PTI, and ETI) pathway marker genes in all AhSBT1.7-transgenic tobacco and *A. thaliana* resistance lines than the susceptible, non-transgenic control plants after pathogen inoculation. But ICS1 in SA signaling showed rapid upregulation at 48 h post inoculation (hpi) and PDF1.2 in JA signaling upregulation at 24 hpi then downregulation compared with that of controls. Interestingly, ERF1 demonstrated a gigantic upregulation of over 35 to 150 folds at 48 hpi, indicating ethylene signaling may be involved in the resistance.

However, PME4, PME2 relating to cell wall metabolism downregulated expressions in the same conditions (Figure S7). Thereby, these signaling pathways may be associated with AhSBT1.7 resistance.

The AtSBT1.7 has been shown to affect the activity of PME in *A. thaliana* (Saez-Aguayo et al., 2013). Furthermore, we assayed PME enzyme activity in *R. solanacearum*-inoculated peanut and found that PME activity increased in

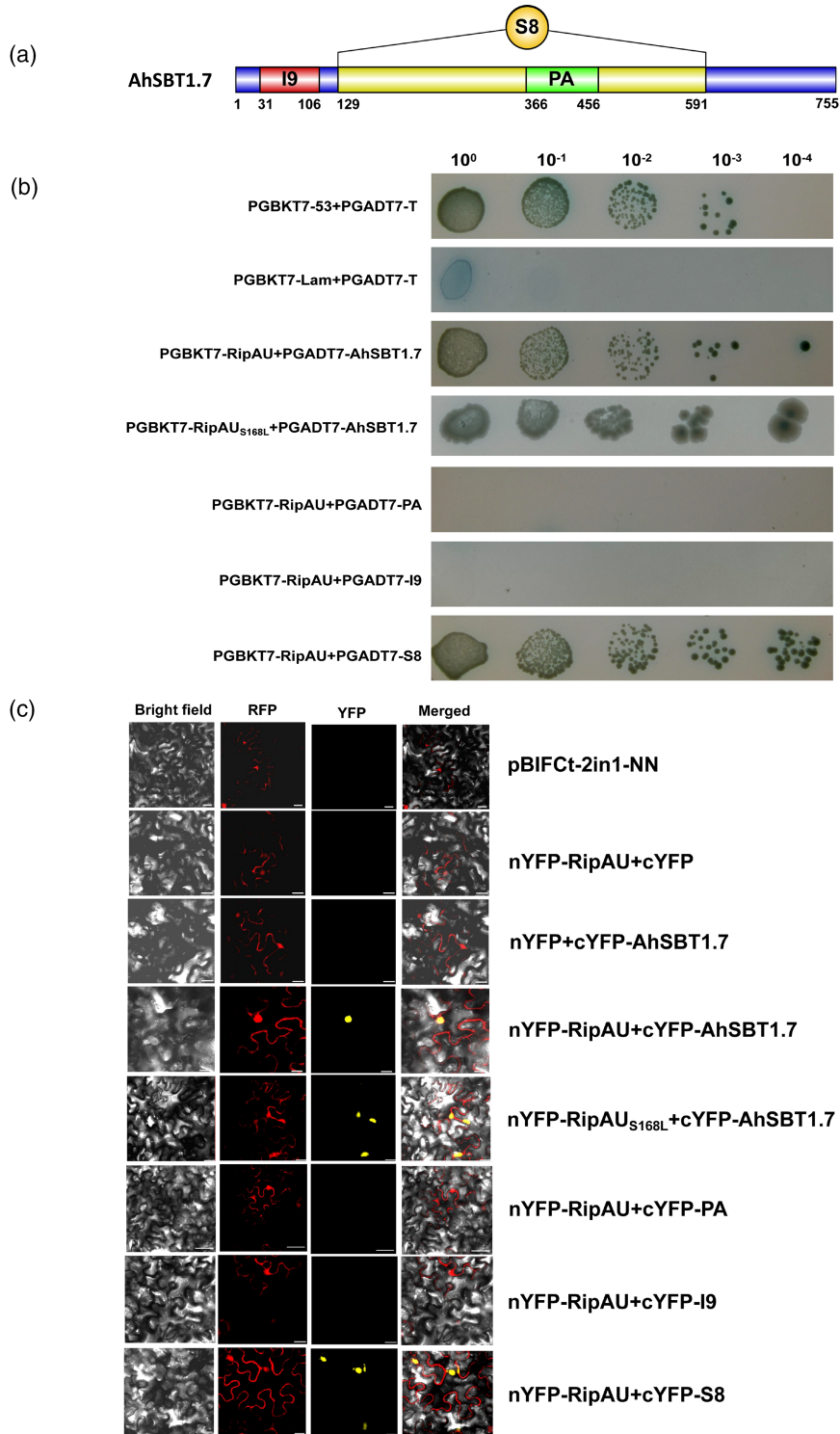
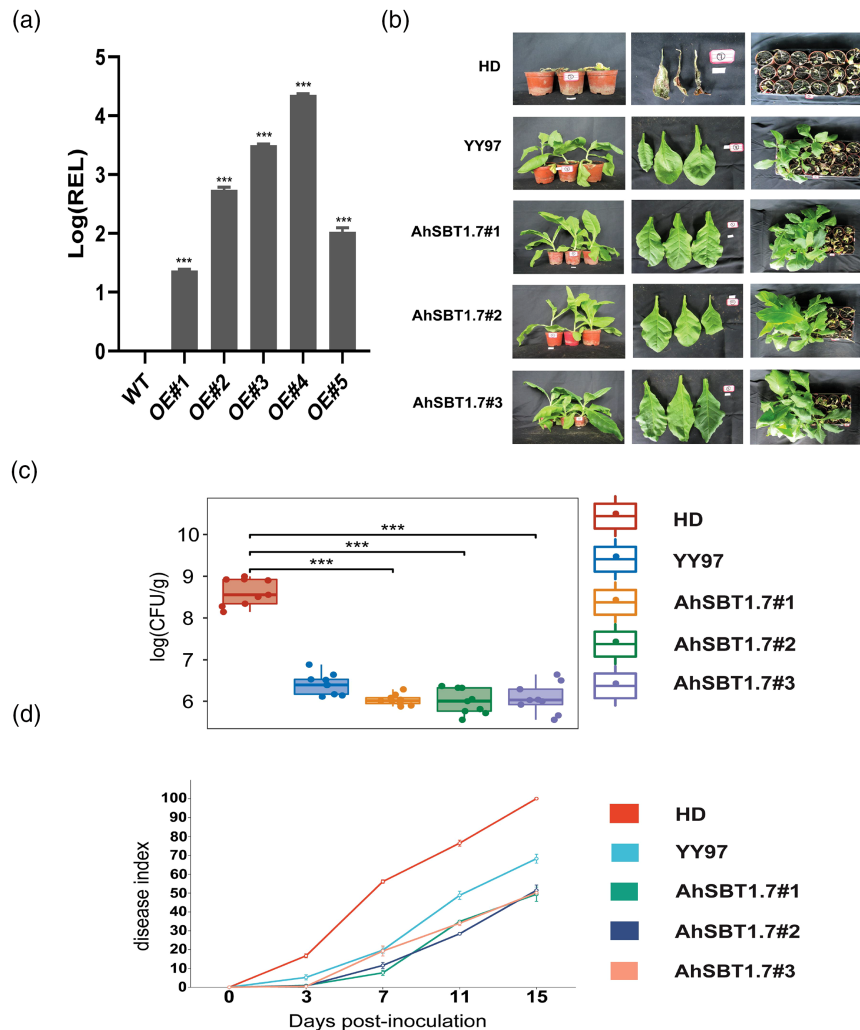


Figure 3. RipAU interacts with subtilisin-like protease SBT1.7.

(a) Schematic representation of the conserved domains on AhSBT1.7 protein.

(b) Yeast two-hybrid validation of the interactions between RipAU or RipAU_{S168L} and AhSBT1.7 full length, its different truncated conserved domain fragments, PA, I9 and S8. pGBKT7-53 + pGADT7-T, the bait and prey containing vector, is used as the positive control; pGBKT7-Lam + pGADT7-T is the negative control. Both RipAU and RipAU_{S168L} can interact with AhSBT1.7 full length proteins. RipAU can only interact with truncated domain S8 of AhSBT1.7, but not with PA and I9 domain fragments.

(c) Ratiometric bimolecular fluorescence complementation experiments (rBIFC) (T UniProt Consortium, 2018) to verify the interaction between proteins. The results are the same with Y2H. The empty vector pBIFCt-2in1-NN contains RFP as control. nYFP or cYFP with on protein used as negative control. Only they merged with RipAU/RipAU_{S168L} and SBT1.7, respectively, they interacted with each other. Bar = 25 μ m.

**Figure 4.** Functional identification of the AhSBT1.7 gene.

(a) Relative expression levels of AhSBT1.7 in different transgenic lines of tobacco HD. All transgenic tobacco HD expressed AhSBT1.7 transcripts while the WT did not express any AhSBT1.7 transcript. REL: relative expression level ($n = 3$).

(b) Phenotype observation of susceptible tobacco HD overexpressing AhSBT1.7 and the nontransgenic resistant YY97 control plants. #1, #2, and #3 represented different transgenic lines, and all transgenic plants were identified at the T2 generation. Photos were taken at 2 weeks post-inoculation (PI) at 28°C. Comparison of *Ralstonia solanacearum* colonization levels in tobacco stems was calculated at 3 days PI ($n = 9$, t -test, $***P < 0.001$).

(c) The disease index of tobacco inoculated with pathogen were calculated 2 weeks PI using formula: $D = \Sigma(M_i \times S_i) \times 100 / (N \times 9)$, explained in the text.

response to the wild type pathogen, maxing out at 48 h, and then slowly decreased to original level (Figure 5a). In contrast, there was no significant change in the PME

activity after inoculating the Δ RipAU mutant strain (Figure 5a), indicating that PMEs may involve in RipAU pathogenicity. At the same time, we also measured the

activity of PME genes in *AhSBT1.7* transgenic plants and found that overexpressing *AhSBT1.7* significantly inhibited *in vivo* PME protein activity in tobacco and *A. thaliana* all the time points from 0 to 96 h post pathogen inoculation compared with the non-transgenic control plants (Figure 5b,c), indicating that *AhSBT1.7* should inhibit PME

activity for immunity. To confirm the speculation, we applied exogenous PME on *A. thaliana* roots and found that the susceptibility of *A. thaliana* to *R. solanacearum* was more serious with the concentration of irrigated PME solution increased (adding 5 ml, from 5 to 25 U ml⁻¹) (Figure 5d; Figure S7c). All these results indicate that the

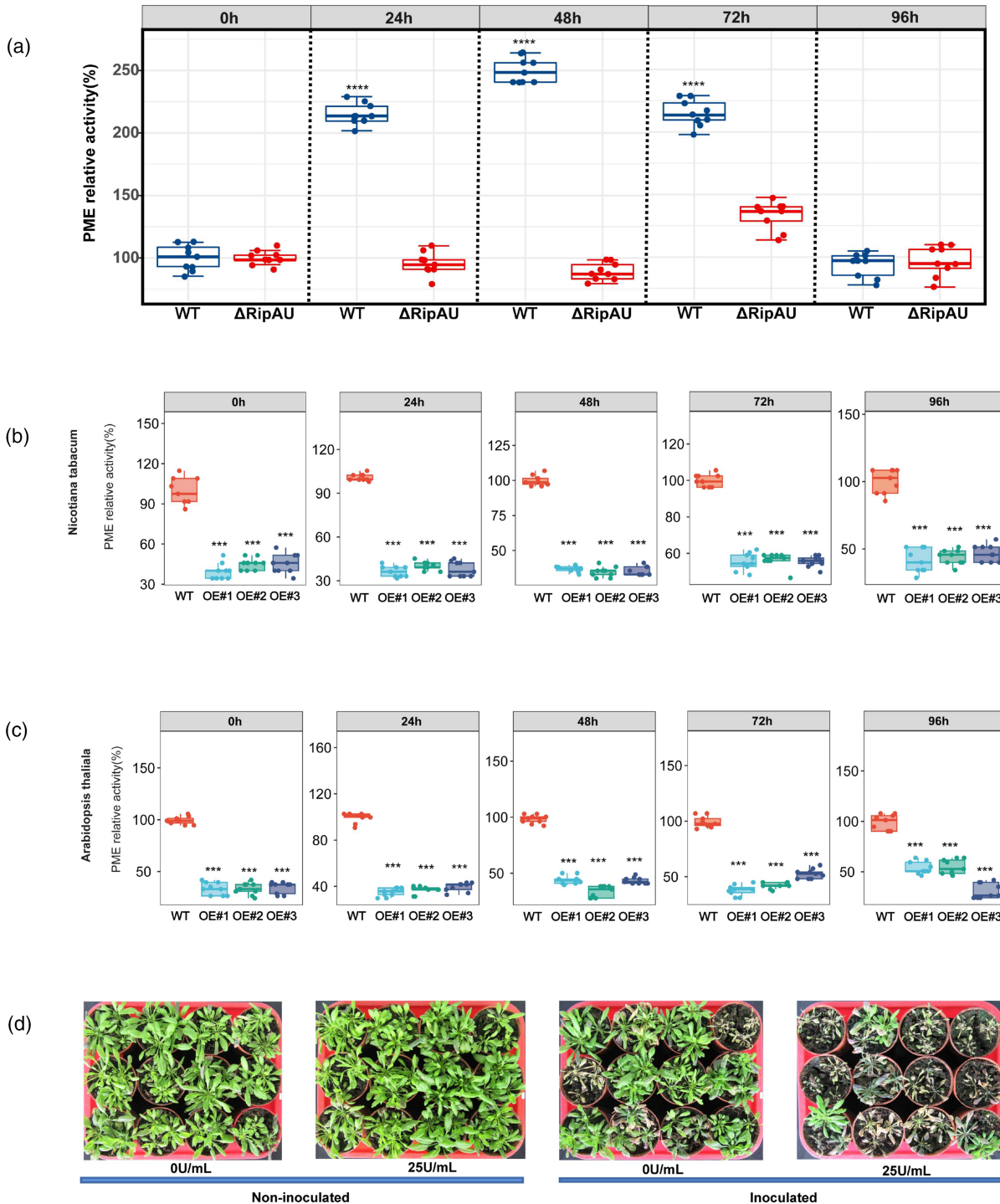


Figure 5. The activity of PME in plants associated with RipAU and AhSBT1.7.

- (a) The PME activity of susceptible peanuts XHXL, inoculated with wild-type and Δ RipAU *Ralstonia solanacearum*, respectively, showed upregulation then returned to original status at different time points of RipAU inoculation ($n = 9$, t-test, $***P < 0.001$; $****P < 0.0001$).
- (b) The PME activity of AhSBT1.7 overexpression *N. tabacum* lines kept low expression at different time points after wildtype *R. solanacearum* inoculation. Samples were taken at different time points after tobacco was inoculated with *R. solanacearum* to measure the PME activity ($n = 9$, t-test, $*P < 0.05$; $***P < 0.001$).
- (c) The PME activity of AhSBT1.7 overexpression *Arabidopsis thaliana* lines was low all the time with wildtype *R. solanacearum* inoculation. After *R. solanacearum* was inoculated into transgenic Arabidopsis, samples were taken at different time points to measure the PME activity ($n = 9$, t-test, $***P < 0.001$).
- (d) Increased exogenous PME application impaired the plant disease resistance. Five millilitres of PME of different concentrations was taken to irrigate Arabidopsis, and then inoculated with *Ralstonia solanacearum* 24 h later. The plants were observed and photographed 1 week later ($n = 27$).

PME may involve in the pathogenicity of RipAU but subjected to the expression of AhSBT1.7.

RipAU transcriptionally regulates various metabolic pathways

To investigate the metabolic pathways affected by RipAU in peanut, an RNA-Seq analysis of *R. solanacearum*-inoculated XHXL with RipAU or no (Δ RipAU) showed that RipAU differentially regulates 2804 common genes across the four time points after inoculation (Figure 6a–e; Table S2). KEGG analysis revealed that most of these differentially expressed genes (DEGs) enriched the phenylpropane metabolic pathway at the four time points, affecting phenylpropane biosynthesis (Figure 6f; Table S3). Moreover, some DEGs enriched the biosynthesis of plant hormones such as SA, IAA, ABA, and PTI signal transduction (Figure S8; Table S4). RipAU downregulated most IAA, SA, and ABA signaling genes and upregulated PTI-related genes. RipAU inoculation decreased the expression of many disease-resistance genes, mainly R and defense-related genes. Importantly, nearly all AhSBTs were downregulated by RipAU (Figure S8; Table S4). Therefore, RipAU impaired R genes and hormone signaling to institute its virulence in peanut. The transcriptome of WT (with RipAU) and Δ RipAU-inoculated peanuts revealed 35 differentially expressed PME genes in peanut (22 genes upregulated and 13 downregulated), confirming the involvement of PMEs in RipAU pathogenicity (Figure S8c; Table S5). The 13 PMEs probably support AhSBT1.7 associating the activity of endogenous PMEs. A qRT-PCR analysis of ten selected candidate DEGs showed consistent expression with the RNA-Seq results (Figure S9).

A WGCNA analysis identified 21 co-expression modules using different color codes, with co-expressed genes clustering into the same module (Figure 7a; Table S6). The weight values were calculated using the soft threshold function in the WGCNA package (Langfelder & Horvath, 2008), and when the fitted curve first approached 0.9, a soft threshold $\beta = 14$ was determined (Figure 7b). The top 10 genes in each module were regarded as hub genes (Table S7).

Thus, functional annotation of these hub genes of modules revealed three modules (deepink1, darkviolet,

and navajowhite2) whose hub genes are related to plant immunity (Table S7). Interestingly, AhSBT1.7, the RipAU target gene, was the first hub gene in the deepink1 module, and this module contained three hub genes belonging to the AhSBTs gene family (Table S7). These AhSBTs genes jointly regulate other genes in this module. Two genes in the darkviolet (AH16G08890: Pectin acetyltransferase, AH17G23980: Endoglucanase) module and three in the navajowhite2 module (AH10G20860: Subtilisin-like protease SBT1.8, AH04G14810: Glucan endo-1,3-beta-glucosidase, AH03G06730: Transcription factor RF2b) are related to plant immunity (Table S7). These results conformed with the transgenic studies. We visualized the co-expression network of these genes with Cytoscape 3.9.0 (Figure 7c; Figure S10). It showed that there were 69 genes associated with the hub gene of subtilisin-like protease in peanut with 31 upregulated expressed genes (FC >1.5) (Figure S6g; Table S8). Moreover, RipAU affected negatively the relative expression of AhSBT1.7 (Figure S9). These results confirmed that AhSBT1.7 should be involved in the RipAU biological processes contributing the immune response in peanut, particularly the PME cell wall degrading pathway.

The AhSBT1.7-targeted AhPME4 participates in RipAU pathogenicity

AhSBT1.7 affects PME activity in transgenic plants, but whether AhSBT1.7 directly or indirectly affects the PME activity is still unknown. Δ RipAU significantly downregulated seven PME family genes (Table S5), suggesting that these seven genes are potential AhSBT1.7 targets. These genes exhibited diversity in their conserved domains and three-dimensional structures (Figure S11a,b). Through Y2H and the BIFC investigation, it definitely proved the AhSBT1.7 did interacted with AhPME4, whereby AhPME4 is the direct target of AhSBT1.7 (Figure 8a,b).

PME is a cell wall degrading enzyme that can destroy plant cell walls (Wang et al., 2020), making it easier for pathogens to infect plants (Figure 5d). We further inoculated *R. solanacearum* after transiently expressing AhPME4 on *N. benthamiana* leaves for 48 h. It was found that tobacco leaves transiently expressing AhPME4 withered

obviously, while the control leaves had no wilt phenotype at the same time (Figure 8c). We determined the colonization of *R. solanacearum* in *N. benthamiana* leaves, and the

results showed that the transient expression of *AhpPME4* increased the colonization of *R. solanacearum* in the host (Figure 8d). The results approved that *AhpPME4* is a

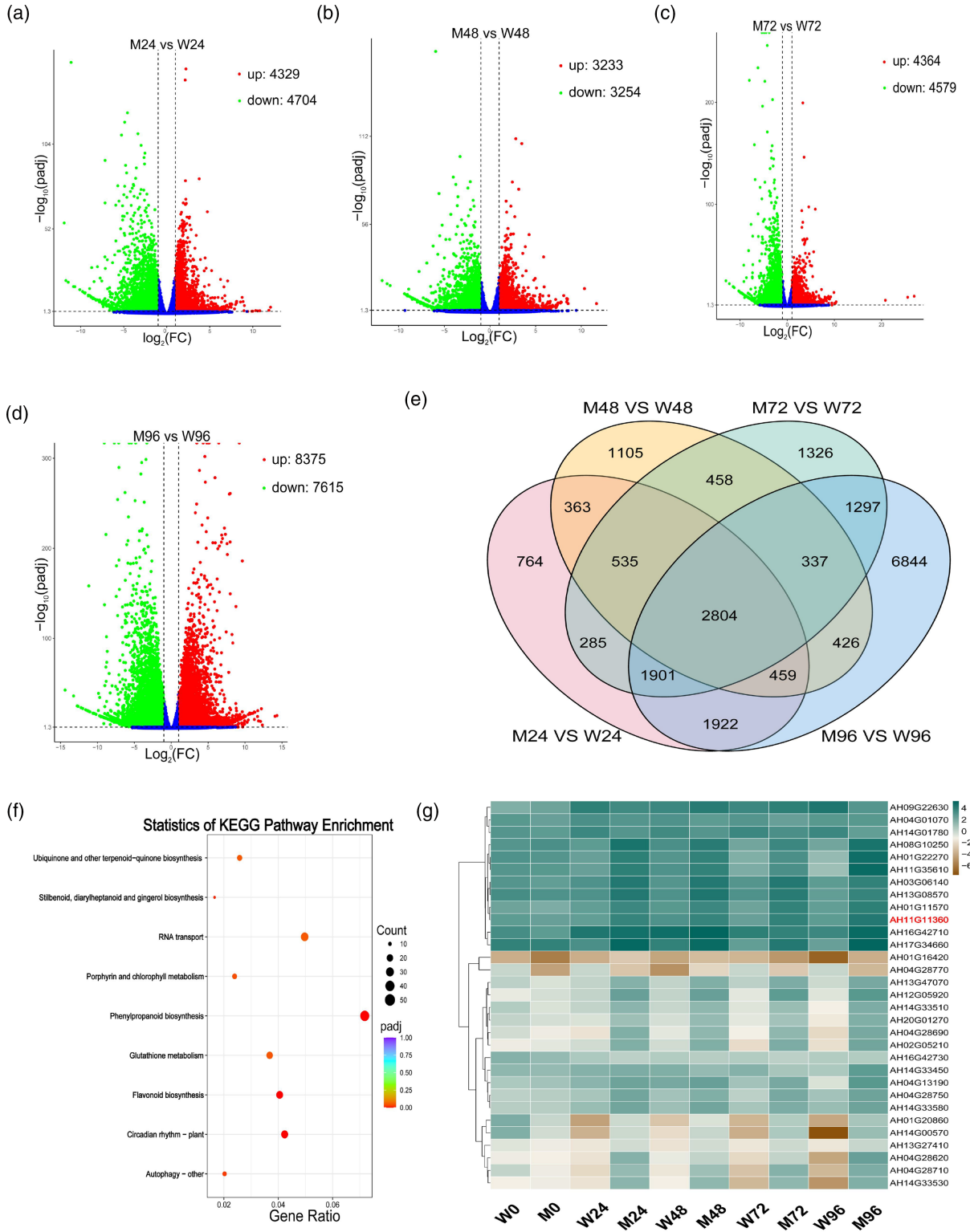


Figure 6. Transcriptional changes in peanut after *Ralstonia solanacearum* infection.

- (a) The volcano plot of differentially expressed genes (DEGs) at 24 hpi.
 (b) The volcano plot of DEGs at 48 hpi.
 (c) The volcano plot of DEGs at 72 hpi.
 (d) The volcano plot of DEGs at 96 hpi. Each point in the figure represents a gene, where red indicates upregulated genes, green indicates downregulated genes, and black indicates nondifferential genes.
 (e) Distribution of DEGs at different stages. The Venn diagram was drawn by Primer3 software (Untergasser et al., 2012).
 (f) KEGG enrichment analysis of DEGs. The vertical axis represents different KEGG signaling pathways, and the horizontal axis represents gene ratio.
 (g) Expression levels of the *AhSbt1.7* gene family at different stages after W and M strains inoculation. Almost all SBT1.7 genes showed upregulation with Δ RipAU mutant strain inoculation. W represents pathogens with RipAU wild genotype, while M represents Δ RipAU. Green indicates upregulated expression, and brown indicates downregulated expression. The greener the color, the higher the upregulation fold, and the browner the color, the higher the downregulation fold.

susceptible gene, which is conducive to the infection of *R. solanacearum* in tobacco leaves.

To know RipAU pathogenicity correlated with *AhPME4* and *AhSBT1.7*, transient expressions of the both genes were performed in *N. benthamiana*. It showed individual expression of *AhPME4* only increased the activity of the PME enzyme, and *AhSBT1.7* significantly inhibited the *AhPME4*-induced activity (Figure 8e) when co-expression with *AhPME4*. However, *RipAU* co-expression with *AhPME4* did not change *AhPME4*-induced activity indicating no direct interaction or inhibition. Co-infiltration of RipAU, *AhSBT1.7*, and *AhPME4* significantly increased the activity of PME compared with that of *AhSBT1.7* and *AhPME4* co-expression (Figure 8e), which definitely showed that RipAU increases PME activity by targeting and reducing the *AhSBT1.7* inhibition of *AhPME4* for its pathogenicity.

DISCUSSION

RipAU inhibits *AhSBT1.7* triggering the pathogenicity of *R. solanacearum*

RipAU is among the most virulent effectors as the Δ *RipAU* strain completely lost its pathogenicity to peanut, and *CRipAU* restored its original wild-type toxic level of pathogenicity. RipAU largely coevolved with the *R. solanacearum* phylotypes. Transiently expressing *RipAU* in tobacco-induced cell death, but the RipAU in GMI1000 did not (Niu et al., 2021). The RipAUs sequence diversity was found between Rs-P.362200 and GMI1000 (Figure 2d). Experiments of site-specific mutations showed that the serine site mutation, S168L, causes RipAU to lose cell death in Rs-P.362200 (Figure 2e), and so for the RipAU in GMI1000, but the SNP did not change its target interaction and the pathogenicity. The peanut cDNA library screened by Y2H obtained that *AhSBT1.7* was the RipAU target protein, confirmed by Y2H and BiFC assays, and conformed with RNA-seq result. It was known that the SBTs, a serine protease, widely involved in plant defense (Figueiredo et al., 2014), and RNA-seq showed RipAU inhibited *AhSB1.7* for its pathogenicity. The *AhSBT1.7* localized at the cell wall and cytoplasmic membrane, whereas RipAU

localized in the nucleus and cytoplasm. In contrast, the *AhSBT1.7* and RipAU interaction complex was mutually localized to the nucleus, indicating that the RipAU-*AhSBT1.7* interaction may change host transcriptions and inhibit function of *AhSBT1.7* for its pathogenicity. This conclusion could be confirmed by the evidence of *AtSBT5.2* in Arabidopsis (Serrano et al., 2016) and the RNA-seq results.

RipAU interferes with the transcriptional regulation of various metabolic pathways

Transcriptome analysis showed that RipAU differentially regulated 2804 peanut genes including *AhSBT1.7*. The 2804 DEGs included R genes (for disease resistance), genes for hormone signaling, including ABA, SA, and IAA (relating to plant growth and defense), and significantly downregulated almost all *AhSBT* family genes (Figures S8 and S9; Figure 6g). These changes led to the observed bacterial wilt disease (Figure 1b–d). Moreover, WGCNA analysis identified 21 co-expression modules, and *AhSBT1.7* as a hub gene for response to RipAU (Figure 7c; Table S7), indicating that *AhSBT1.7* is a key player in RipAU pathogenicity. Subtilisin-like proteases, including *AhSBT1.7*, are serine proteases with highly specific functions in plant development and signaling pathways (Figueiredo et al., 2014). The *AtSBT1.3* and *AtSB5.2* trigger innate immune responses in *A. thaliana* against *Pseudomonas syringae* (Ramirez et al., 2013). Besides, *GbSBT1* enhances resistance to *F. oxysporum* and *V. dahliae* infection in cotton (Duan et al., 2016). Altogether, these results confirmed that *AhSBT1.7* is an immune-response gene. The RipAU pathogenicity depends on targeting and inhibiting *AhSBT1.7* to impair plant immune responses.

AhSBT1.7 inhibits PME activity to enhance the resistance

Transgenic tobacco and *A. thaliana* overexpressing *AhSBT1.7* significantly enhanced the resistance against *R. solanacearum*. Besides, transgenic tobacco overexpressing *NbSBT1.7* also demonstrated high resistance to bacterial wilt. This concluded that *SBT1.7* is the key plant resistance gene for immunity against *R. solanacearum*. A qRT-PCR characterization of transgenic lines showed that

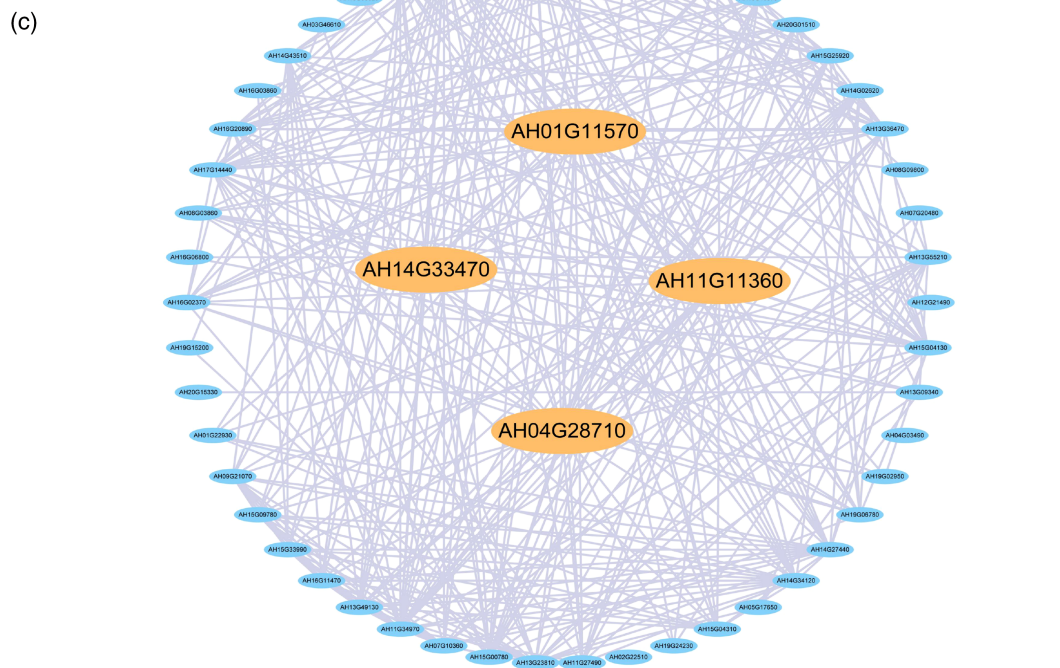
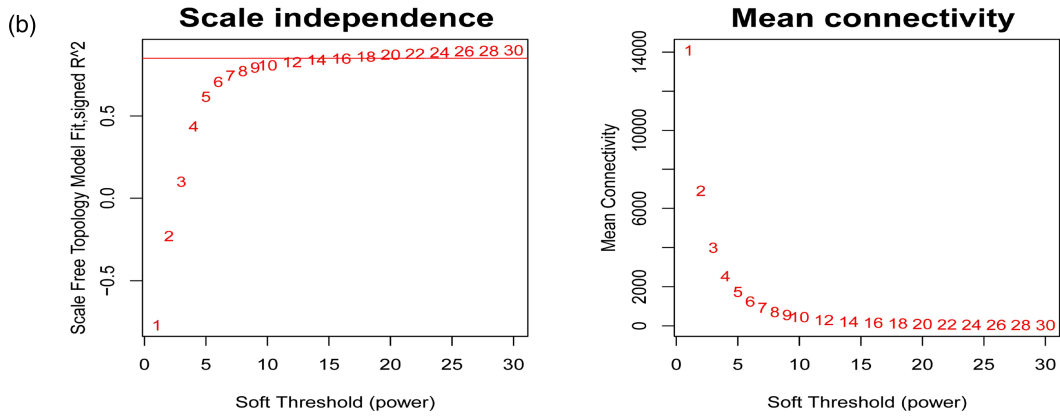
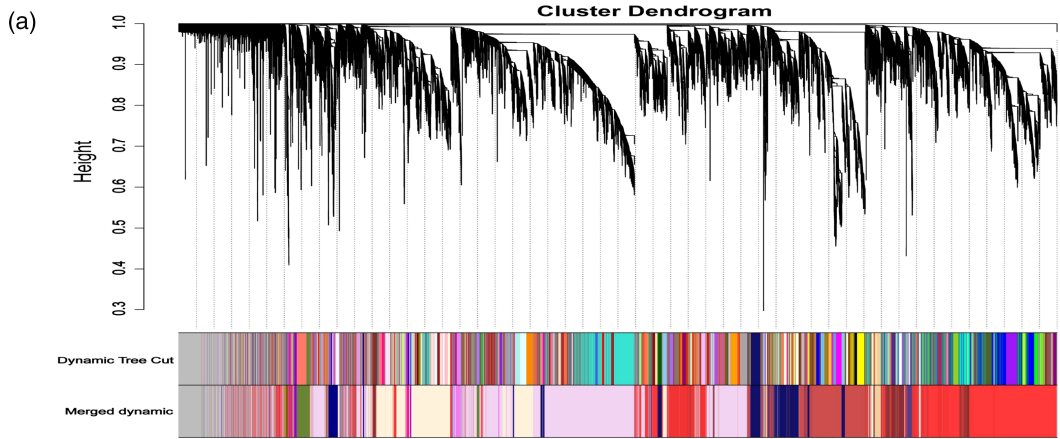
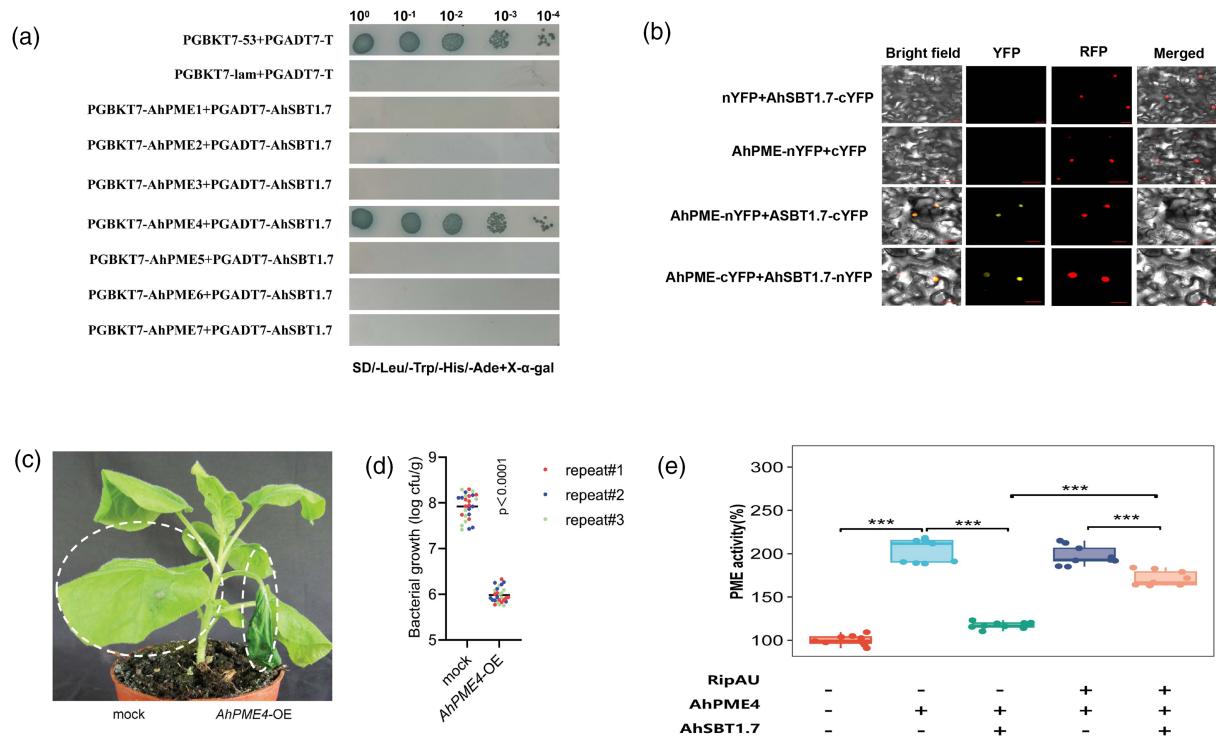


Figure 7. WGCNA of genes in with *Ralstonia solanacearum*-inoculated peanut at different DPI.

(a) Gene cluster dendrograms and module detecting.

(b) Soft threshold determination.

(c) Co-expression network related to AhSBT1.7 (AH11G11360). The weighted gene co-correlation network analysis (WGCNA) was performed using the WGCNA R (version 4.0.3) package (Figueiredo et al., 2014). Network of co-expressed genes was visualized using Cytoscape 3.9.0 (Saito et al., 2012).

**Figure 8.** Interaction of AhPME4 with AhSBT1.7 and RipAU pathogenicity signal characterization.

(a) Y2H validation of the interaction between AhSBT1.7 and AhPME4. AhPME4 was constructed into pGBKT7, and AhSBT1.7 was constructed into pGADT7, which were transformed into the yeast strain Y2H Gold, and the protein interaction was verified by the yeast screening system.

(b) BIFC validation of the interaction between AhSBT1.7 and AhPME4. AhSBT1.7 and AhPME4 were constructed into the vector pBIFCt-2in1-NN, transiently expressed in tobacco by *Agrobacterium* for 48 h, and observed and photographed using a laser confocal microscope (20 \times). The empty vector pBIFCt-2in1-NN contains RFP as control. nYFP or cYFP with on protein used as negative control. Bar = 25 μ m.(c) The transient expression of AhPME4 shows an increased susceptibility to *Ralstonia solanacearum* with significantly higher propagation 3 days after inoculating the tobacco leaves.(d) Bacteria growth in *Nicotiana benthamiana*. Three days after the inoculation of *R. solanacearum*, 1 g of plant stems was weighed, added with an appropriate amount of sterile water and ground, and then the bacterial content was calculated in the culture medium by the gradient dilution method.(e) Different combinations of RipAU/AhPME4/AhSBT1.7 transient co-expression in *Nicotiana benthamiana* for 48 h regulated diverse PME enzyme activity (n = 9, t-test, ***P < 0.001).

AhSBT1.7 resistance is associated with the expression changes of SA, JA, R genes, ET and PME signaling, mainly activating ERF1 and inhibiting PME pathway (Figure S7). All AhSBT1.7-transgenic tobacco or *A. thaliana* plants inhibited PME activity with or without pathogen inoculation (Figure 5b,c). PME is a cell wall degrading enzyme that mainly catalyzes pectin demethylation (Huang et al., 2022). AtSBT1.7 reportedly alters the mechanical properties of cell wall mucilages and inhibits pectinesterase activity in *A. thaliana* by activating the PME inhibitor or inactivating PME through proteolysis (Saez-Aguayo et al., 2013). These properties confirmed that AhSBT1.7 transgenic lines

maintained intact plant cell walls while control plants displayed degraded cell walls and rotten roots (Figure S4). Therefore, AhSBT1.7 regulates plant resistance by inhibiting PME and activating defense signaling genes.

AhPME4-mediated cell wall degradation was inversely regulated by AhSBT1.7 and RipAU

PMEs were known to regulate the pectin methylesterification status leading plant cell wall stiffening or loosening to degradation (Saez-Aguayo et al., 2013; Silva-Sanzana et al., 2019), and cell wall degradation is the distinct characteristic of *R. solanacearum* infection in plant roots. In the

study, AhPMEs were found involved in RipAU pathogenicity mostly as upregulated genes by the transcriptome and qRT-PCR analysis (Figures S8c and S9), and the PME_s were inhibited by *AhSBT1.7* transgenic tobacco and *A. thaliana* lines, also confirmed in the *NbSBT1.7* overexpression lines (Figure S7a–c). These indicated PME played roles in RipAU pathogenicity modulated independently by RipAU and *AhSBT1.7* in contrary directions. Application of exogenous PME made tobacco plants more susceptible to *R. solanacearum*, dynamically confirmed PME promotes pathogenicity. Furthermore, transient expression of the RipAU-upregulated *AhPME4* in *N. benthamiana* increased disease susceptibility (Figure 8c,d). These indicated *AhPMEs* acted downstream of *AhSBT1.7* led to plant bacterial wilt via degradation of cell wall. By Y2H and BiFC, the PME4 showed direct interaction with *AhSBT1.7*, demonstrating *AhSBT1.7* targets *AhPME4* for its resistance. This confirmed with the hypothesized that *SBT1.7* could regulate the methylesterification degree of pectin homogalacturonan through the degradation of PME or activation of PME1 by limited proteolysis (Rautengarten et al., 2008; Saez-Aguayo et al., 2013). Interestingly, the two interacted proteins also mutually localized at nucleus (Figure 8b; Figure S11c), implying that the *AhSBT1.7* should partially degrade the PME4 to change the activity and localization and the expressions for its immunity. This was different from the previous report (Saez-Aguayo et al., 2013). However, in *A. thaliana* AtPMEs were reported to increase immunity of resistance to *P. syringae* and it was believed caused by some specific PME_s (Bethke et al., 2014). Furthermore, co-transient experiments on *N. benthamiana* definitely confirmed that the *AhPME4* activity required for degrading cell wall for the RipAU pathogenicity was inhibited by *AhSBT1.7* but upregulated by RipAU via prohibit the *AhSBT1.7* (Figure 8e). The results reveal the mechanism of RipAU modulated pathogenicity and its host interaction leading to bacterial wilt disease.

A model for RipAU-*AhSBT1.7* interaction to control *R. solanacearum* pathogenicity

Current research on T3Es has focused on model plants such as *A. thaliana* (Yu et al., 2022), potatoes (Zheng et al., 2019), and tomatoes (Caiying et al., 2021). Nonetheless, target genes and pathogenic mechanisms of T3Es in peanuts remain unknown. Our study has shown that the pathogenicity of *R. solanacearum* to peanut was lost after the knockout of RipAU. Y2H and BiFC defined the target gene of RipAU in peanut is *AhSBT1.7* that localized with effector RipAU in nucleus after the interaction, implying RipAU interacts with *AhSBT1.7* to change transcriptome for pathogenicity. Although *AhSBT1.7* contains cell wall-localized signal peptide on the N-terminal, it should interact with RipAU inside the cell, as all plant proteins are first synthesized by the ribosomes associated with endoplasmic

reticulum and may be processed there (Weis et al., 2015), then sorted to different cell parts via the Golgi apparatus (Otegui et al., 2024). After RipAU interacts with *AhSBT1.7*, it may change the *SBT1.7* structure or modify it, then changes its location by mutual relocalization at the nucleus to change the host expressions, which were often seen by previous research (Nemes et al., 2017; Qiao et al., 2012; Sasaki et al., 2018). RNA-Seq analysis confirmed that RipAU induced 2802 DEGs including inhibiting *AhSBT1.7* expression, while WGCNA analysis coincidentally revealed that *AhSBT1.7* was a hub gene in participating pathogenicity (Figure 7). Heterologous expression of *AhSBT1.7* in tobacco and Arabidopsis enhanced plant tolerance to *R. solanacearum*, confirming that this gene is a critical gene during plant immunity. We showed *AhSBT1.7* induced *ERF1* expression and suppressed cell wall degrading protease PME expression for its defense. Enzymatic activity experiments proved that PME activity was significantly reduced in transgenic plants. We also demonstrated the interaction between *AhSBT1.7* and *AhPME4* and *AhSBT1.7* can inhibit the expression of *AhPME4* (Figure 8). Subsequently, we further revealed that *AhPME4* promote plant susceptibility by degradation cell wall which is inversely regulated by RipAU and *SBT1.7*. By the same mechanism, the *AhSBT1.7* should interact with *AhPME4* inside the cell being both synthesized or processed within. The RipAU might targets *AhSBT1.7* to impair its interaction with *AhPME4* for its pathogenicity, which needs further studies. In conclusion, we generalized a model as in Figure 9. It showed that after T3SS secreted RipAU into the host, the interaction of RipAU and *AhSBT1.7* in nucleus inhibited the transcription of R genes, SA, ABA, and IAA signaling genes and the *AhSBT1.7* themselves. Moreover it increased the activity of PME, promoting cell wall degradation in the host, thus making the host plant susceptible (Figure 9). Therefore, we revealed the function of *AhSBT1.7* and PME in disease resistance and elucidated the pathogenic mechanism of RipAU.

MATERIALS AND METHODS

Plant growth and treatment

The study used two peanut cultivars, Xinhui Xiaoli (XHXL) and Yueyou 92 (YY92), which are highly susceptible and highly resistant to *R. solanacearum*, respectively. The Center for Legume Plant Genetics and Systems Biology, Fujian Agriculture and Forestry University, maintained the cultivars. Peanut seeds were sown in plastic pots containing nutrient soil and maintained in the greenhouse at 28°C. *R. solanacearum* inoculation was performed when the peanut seedlings reached the four-leaf stage.

The functions of the target genes were studied using two tobacco varieties, one highly susceptible variety Honghuadajinyuan (HD), and a highly resistant variety, Yanyan 97 (YY97), to *R. solanacearum* FJ1003. The seeds of HD and YY97 were vernalized at 4°C for 2 days before sowing. One week later, the seedlings were transplanted into pots containing nutrient soil for

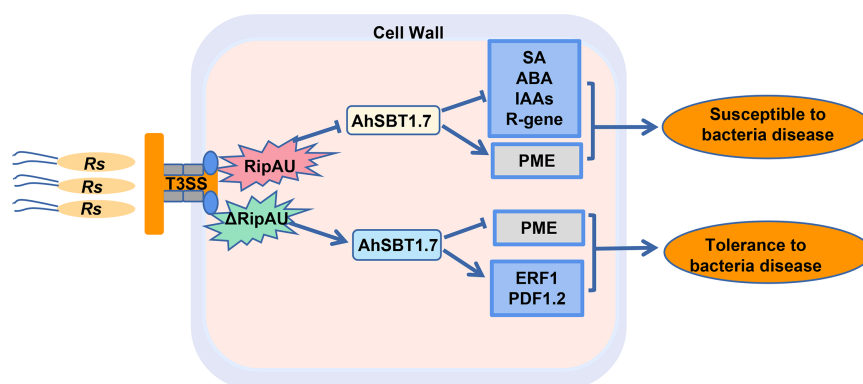


Figure 9. Working model for the pathogenic mechanism of RipAU. AhSBT1.7 is a disease-resistance gene, and the resistance is PME-mediated involvement. RipAU targets and inhibits AhSBT1.7, thereby downregulating SBT.7 gene defense and other resistance signal pathways, and increasing PME content, which leads to host susceptibility.

4 weeks. *A. thaliana* (Col-0) plants were also used for evaluation of target gene function and were grown in the greenhouse at 23°C for inoculation using *R. solanacearum* GMI1000. Afterward, the 4-week-old *N. benthamiana* plants were inoculated with *R. solanacearum* used for the cell death response study at 25°C. Besides, the model plant, *N. benthamiana*, was seeded after vernalization and cultured in a greenhouse at 25°C. All plants were grown under 75% relative humidity and 8/16 dark/light cycle.

Generation of *R. solanacearum* mutant and complementary strains

Ralstonia solanacearum Rs-P.362200 (a highly pathogenic strain) was isolated from the main peanut-producing areas of Fujian Province, China (Chen et al., 2021). Specific RipAU primers were designed upstream of the start codon (U) and downstream of the stop codon (D) on the genomic sequence of *R. solanacearum* Rs-P.362200. The PCR products were obtained by gel purification, and U and D fragments were ligated into the pK18mobsacB suicide vector using corresponding restriction enzymes and the T4 DNA ligase. The ligation product was transformed into *Escherichia coli* (DH5 α), and the positive clones were verified by PCR and sequencing. The T3Es knockout vector, pK18mobsacB-U-D, was constructed, the plasmid was transformed into *R. solanacearum* Rs-P.362200, and the target gene was replaced by homologous recombination to obtain the T3Es mutant, strain Δ T3Es.

Specific primers were designed to amplify the upstream U, RipAU, and downstream D fragments of the target *R. solanacearum* genomic DNA to construct the complementary vector. The corresponding restriction enzymes digested the target fragments and emptied the pK18mobsacB vector. Next, U-RipAU-D was ligated into the pK18mobsacB vector using T4 ligase to construct the RipAU complementary vector pK18mobSacB-U-RipAU-D. The pK18mobSacB-U-RipAU-D plasmid was transformed into *R. solanacearum* Δ RipAU, and the target gene was complementary into *R. solanacearum* Δ RipAU by homologous recombination to obtain T3Es complementary strain CRipAU. A schematic diagram of the knockout generation and T3Es complement strains is shown in Figure S12. The primers used in this experiment are provided in Table S9.

Measurement of motility and growth rate

Ralstonia solanacearum P.362200, Δ T3Es, and CT3Es were cultured in bacteria peptone glucose (BG) liquid media (peptone

1.0%, yeast extract 0.1%, casamino acid 0.1%, glucose 1.0%, and agar 1.4%, pH 7.4) at 28°C and 250 rpm. Next, 1 μ l of the bacterial solution ($OD_{600} = 0.5$) was cultured on an SMM semi-solid medium (glucose 0.1%, peptone 1.0%, agar 0.325%, hydrolyzed caseins 0.1%, pH 7.4) at 28°C. The growth of bacterial colonies was observed, and the diameter of each colony was measured every 24 h. *R. solanacearum* was cultured to obtain $OD_{600} = 0.1$, then 100 μ l was drawn into a new centrifuge tube containing 5 ml BG liquid medium, shaken at 28°C, 175 rpm, OD_{600} , and its growth rate was measured after 24 h.

Transient overexpression and subcellular localization analysis

The transient expression vector was constructed using the gateway system. Briefly, the target gene was ligated into the pDONR207 vector by the gateway BP cloning and to the destination vector, pK7WG2.0-GFP, by LR cloning. The transient expression vector was transformed into *Agrobacterium tumefaciens* GV3101, and the positive clones were cultured to OD_{600} of 0.5. Bacterial cells were harvested by centrifugation (1503 g, 10 min), resuspended in MES buffer at 0.7–0.8 OD_{600} , and incubated at 28°C for 2 h. Afterward, three healthy tobacco plants at the 5–6 leaf stage were selected as the experimental group and three as the control group. The penultimate and third leaves of the plants were punctured using a 1 ml syringe needle, and the prepared bacterial solution was injected at the punctured site using the *Agroinfiltration* method. The injection area (up to 1 cm diameter) was encircled, and the allergic necrosis reaction was observed physically within a week. Subcellular localization was observed under a fluorescence microscope.

Pathogenicity identification of *R. solanacearum*

Ralstonia solanacearum was cultured in BG solid medium at 28°C for 2–3 days. A single colony was selected, inoculated on 1 ml BG liquid medium, and cultured overnight. Next, 500 μ l of the overnight bacterium culture was grown up to 0.5 OD_{600} in a 250 ml BG liquid medium, harvested by centrifugation, and resuspended in sterile water up to 0.5 OD_{600} . Then, the leaf-cutting method was used to infect the peanut leaves (Zhang et al., 2017, 2019). Briefly, sterile scissors were dipped into the bacterial inoculum and used to inoculate the 4–6 leaf stage peanut seedlings by cutting the four leaflets of the last three leaves. The disease incidence of peanut plants was recorded daily for 1–2 weeks, and the disease index

was calculated to determine the pathogenicity of *R. solanacearum* using formula: $D = \Sigma(M_i \times S_i) \times 100 / (N \times 9)$, where D indicates disease index; i indicates disease grade; M_i indicates number of plants with i grades; S_i indicates value of i grade. N indicates total plants observed; here 9 indicates the number of grades.

Yeast two-hybrid

The RipAU was ligated in the pGBKT7 vector, and the sequence of the bait vector (pGBKT7-RipAU) was verified accordingly. The pGBKT7-RipAU bait vectors were transformed into yeast AH109, followed by plasmid cDNA library transformation into AH109 (containing pGBKT7-RipAU) and coating on the SD/-His/-Leu/-Trp plate. The clones that grew normally on the SD/-His/-Leu/-Trp plate were transferred to the SD/-Ade/-His/-Leu/-Trp+X- α -gal plate for 2–3 days. Subsequently, clones that turned blue were selected as candidate-positive clones. The plasmids of the candidate positive clones were extracted, verified by PCR, sequenced, and aligned to the Peanut genome resource (<http://peanutgr.fafu.edu.cn/>) to obtain the full-length sequence of the target gene *AhSBT1.7* (ID: AH11G11360). The full-length CDS sequence of *AhSBT1.7* was cloned into the pGADT7 vector, and pGADT7-*AhSBT1.7* + pGBKT7-RipAU was co-transferred. SD/-Leu/-Trp plate was applied for double vector transformants. The SD/-Ade/-His/-Leu/-Trp+X- α -gal plate was observed for 3 days for the colonies that would turn blue, verifying the interaction between RipAU and *AhSBT1.7*. pGBKT7-lam + pGADT7-T was negative control and pGBKT7-53 + pGADT7-T was the positive control.

BIFC experiment

Ratiometric bimolecular fluorescence complementation (rBIFC) was performed following the method of Grefen using the 2in1 vector (Grefen & Blatt, 2012). Briefly, RipAU and the target genes were ligated to P1P4 and P2P3 entry vectors through the Gateway technology, followed by simultaneous ligation into the NN vector using Gateway LR cloning. The genes were transformed using agrobacterium (GV3101), transiently expressed in *N. benthamiana*. Two days later, their interaction was observed and photographed by the confocal microscope.

Phenotyping host susceptibility by *in vivo* bacteria propagation

After *R. solanacearum* inoculation (3/5/7/9 DPI), 1 g of third leaf from transgenic plant or stems between the two inoculated leaves from peanut were precisely sampled, sterilized with 75% alcohol for 30 sec, and washed with sterile water three times for 1 min each. The stem samples were finely ground in 1 ml of sterile water using a sterile mortar and pestle. The supernatant was coated on BG solid medium following the gradient dilution method and cultured at 28°C for 2 days before counting the number of colonies.

Transcriptome analysis

The *R. solanacearum* inoculated peanut leaves were collected at different time points for total RNA extraction using the Trizol reagent (Invitrogen, Carlsbad, CA, USA) following the manufacturer's instructions. The cDNA libraries were constructed using the Illumina paired-end sample prep kit and sequenced on the Illumina HiSeq 2500 platform (Illumina, San Diego, CA, USA). The raw sequencing data were filtered to remove adapters sequences, and low-quality reads to obtain clean reads. These clean reads were mapped to the peanut reference genome using Bowtie v.1.0.0 (Langmead et al., 2009), and

only perfectly matched reads were used for downstream analysis. The DEGs were functionally annotated using COG (Tatusov et al., 2000), KEGG (Kanehisa, 2004), GO (Ashburner et al., 2000), Swiss-Prot (T UniProt Consortium, 2018), and NR (Deng et al., 2006) databases. The gene functions were analyzed using COG, KEGG metabolic pathways, and GO enrichment analysis. Further, a weighted gene co-correlation network analysis (WGCNA) was performed using the WGCNA R (version 4.0.3) package (Figueiredo et al., 2014), and the network of co-expressed genes was visualized using Cytoscape 3.9.0 (Saito et al., 2012).

Phylogenetics analysis

The RipAU protein sequences of different *R. solanacearum* strains were downloaded from NCBI (<https://www.ncbi.nlm.nih.gov/>) and T3Es (<https://iant.toulouse.inra.fr/bacteria/annotation/site/prj/T3Ev3/>) databases. Their evolutionary history was inferred using the Minimum Evolution method (Kumar, 1996). A bootstrap consensus tree with 1000 replicates was constructed to represent the evolutionary history of the analyzed taxa (Felsenstein, 1985). Thus, branches corresponding to partitions reproduced with <50% bootstrap replicates were collapsed. The evolutionary distances were computed using the Poisson correction method (Kaur et al., 2018) and the ME tree was searched using the close-neighbor-interchange (CNI) algorithm (Xia, 2017) at a search level of 1. The neighbor-joining algorithm (Naruya & Nei, 1987) generated the initial tree involving 90 amino acid sequences. All ambiguous positions were removed for each sequence pair, resulting in 552 positions in the final dataset. The evolutionary analyses were conducted in MEGA7 (Kumar et al., 2016).

Genetic transformation of tobacco and Arabidopsis

The *AhSBT1.7* gene was cloned from peanut and constructed into the plant expression vector (pK7WG2.0) using the gateway cloning system. The plant expression vector was transformed to tobacco (HD) following the agrobacterium-mediated genetic transformation (Qin, 2011), and *A. thaliana* plants were transformed following the floral dip method (Xu & Xu, 2018). Finally, the positively transformed tobacco and *A. thaliana* plants of the T1 generation were screened on MS (KM⁺) solid media and verified at the RNA level. The T2 homozygous transgenic lines were used in the follow-up study.

Resistance phenotype identification

Ralstonia solanacearum FJ1003 and GMI1000 were used to inoculate tobacco and *A. thaliana* plants for evaluation of resistance, respectively. *R. solanacearum* was cultured in BG liquid medium until OD₆₀₀ = 0.5, centrifuged, and resuspended in sterile water to make OD₆₀₀ = 0.5. Use root-injury irrigation method for inoculation. Transplanted *A. thaliana* and tobacco transgenic plants were grown for 2–3 weeks, then use a sterile blade to make a "well" shape in the culture bowl to cause mechanical damage to the root. Then each potted plant was filled with 5 ml of resuspension solution and cultured at 28°C. The disease status of the plants is recorded every day and observed for 2 weeks. Calculate the disease index to determine the pathogenicity of *R. solanacearum* using the same formula showed as above.

qRT-PCR

Total RNA was extracted from tobacco and peanut using TRIZOL (Invitrogen) following the manufacturer's instructions. Next, 1 μ g of RNA was reverse transcribed into cDNA using the Evo M-MLV RT Mix Kit (Accurate Biology, Changsha, China) and diluted 5-fold for subsequent experiments. Real-time quantitative PCR was

performed using the ChamQ SYBR qPCR Master Mix (Vazyme, Nanjing, China) with three biological replicates per sample. The peanut actin gene was the internal control, and the relative expression levels of the genes were calculated using the $2^{-\Delta\Delta CT}$ method. The primer sequences used in this study are provided in Table S9.

AUTHOR CONTRIBUTIONS

WZ conceptualized and designed the study. KC performed data analysis and drafted the initial manuscript. KC, YZ, HC, TL, ML, CZ, SW, LW, AB, VG, BJ, RB, RT, and MKP generated or analyzed the different datasets and preparation the figures. HF and LW performed the transcriptome data analysis. WL performed the knockout experiments of some T3Es. WZ and RKV provided the technical guidelines for experimental design, data analysis, and manuscript preparation. All authors have read and agreed on the current version of the manuscript.

ACKNOWLEDGMENTS

We are grateful for the support provided by the National Natural Science Foundation of China (grant numbers: 32401787, 32072103, 31701463 and U1705233), the Chinese Ministry of Science and Technology (2023YFD1202802) and the Technological Innovation of Fujian Agriculture and Forestry University (KFB23002).

CONFLICT OF INTEREST

The authors declare no conflict of interest.

DATA AVAILABILITY STATEMENT

RNA-Seq data reported in this article have been deposited in Peanut Genome Resource (<http://peanutgr.fafu.edu.cn/>). Gene sequence of Subtilisin-like protease (AhSBT1.7, gene ID: AH11G11360) and pectin methylesterase (PME4, gene ID: AH03G21690) have been deposited in Peanut Genome Resource. RipAU (gene ID: 2_1202) sequence have been reported in previous study (Chen et al., 2021). For other data, based on request.

SUPPORTING INFORMATION

Additional Supporting Information may be found in the online version of this article.

Figure S1. Pathogenicity identification of *Ralstonia solanacearum*. Phenotypes of different genotype strains were observed 14 days after inoculation of peanut variety Xinhui Xiaoli. The leaf cutting method was used for inoculation with *R. solanacearum*. The CK inoculated with water as the blank control. CRipAU(S168L) and CRipAU can lead to pathogenicity as WT strain, indicating they can restore the Δ RipAU virulence.

Figure S2. Molecular phylogenetic analysis of RipAU. The phylogenetic tree was constructed by the minimum-evolution method. Different colors represented different phylotypes. Roman numerals indicate the category of phylotypes. The Roman numerals are preceded or followed by the numbers of different *R. solanacearum* sources. The asterisk marks RipAU.

Figure S3. Subcellular localization of RipAU and AhSBT1.7. (a) A schematic of vector construction with interested genes. (b)

Subcellular localization of genes in *N. benthamiana*. RipAU and AhSBT1.7 were constructed into the plant expression vector pK7WGFP and transiently expressed in *N. benthamiana* mediated by *Agrobacterium*. The cells were observed and photographed after 48 h. GFP was used as a blank control, and all images were taken with laser confocal microscope (20 \times). Bar = 25 μ m.

Figure S4. Slices of transgenic tobacco inoculated with *R. solanacearum*. Two weeks after inoculation, tobacco stems were cut off with a scalpel, and the transverse section, longitudinal section, and root phenotypes were observed accordingly (Bar = 0.2 cm).

Figure S5. Functional identification of the AhSBT1.7 gene. (a) Identification of disease-resistant AhSBT1.7-transgenic plants. Fourteen days after the inoculation of *R. solanacearum* on 4–5 week-old *A. thaliana*, observations and photographs were taken. (b) Disease index of AhSBT1.7 overexpression lines and col-0 inoculated with *R. solanacearum*. (c) *R. solanacearum* colonization of tobacco stems. Three days after inoculating *A. thaliana* with *R. solanacearum*, the stems between the penultimate and second leaves were taken, and ground with sterile water, and the number of colonies was calculated by the gradient dilution method ($n = 9$, t -test, $*P < 0.05$; $**P < 0.01$; $***P < 0.001$).

Figure S6. Functional identification of the NbSBT1.7 gene. (a) Identification of the disease resistance of NbSBT1.7 transgenic tobacco lines with nontransgenic susceptible variety HD and non-transgenic high resistant variety YY97 as control. Observation and photography 2 weeks after the tobacco was inoculated with *R. solanacearum*. (b) The disease index of *R. solanacearum*-inoculated tobacco. (c) *R. solanacearum* colonization of tobacco stems. Three days after inoculating tobacco with *R. solanacearum*, the stems between the penultimate and the second leaves were taken, and ground with sterile water, and the number of colonies was calculated by the gradient dilution method ($n = 9$, t -test, $*P < 0.05$; $**P < 0.01$; $***P < 0.001$).

Figure S7. Relative expression of different signaling genes in transgenic plants and PME function characterization. (a) Relative expression of genes affected by overexpressing AhSBT1.7 in tobacco. (b) Relative expression of genes affected by overexpressing AhSBT1.7 in *Arabidopsis*. (a, b, $n = 3$, t -test, $*P < 0.05$; $**P < 0.01$; $***P < 0.001$). (c) Effects of exogenous PME on plant disease resistance. Irrigate the roots with PME solutions (5 ml) of different concentrations, and then inoculate *R. solanacearum* 1 day later.

Figure S8. The differentially expressed genes (DEGs) in peanut inoculated with *R. solanacearum* are related to disease resistance. (a) Clusters of DEGs from peanut XHXL seedlings inoculated with wildtype RipAU (W) or Δ RipAU (M) strains for 0, 24, 48, 72 and 96 h, respectively. (b) DEGs in hormonal and immune signaling pathways at different stages after W and M strains inoculation. (c) Expression of the AhPME gene family in different stages after W and M strains inoculation.

Figure S9. Quantitative RT-PCR validation of selected DEGs with Δ RipAU versus wild type *R. solanacearum*. Values of expression levels are means \pm SE of three replicates ($n = 3$). AhPME2 (AH01G00990, pectinesterase 2), AhPME6 (AH01G00670, pectinesterase 6), AhRPP13 (AH02G00200, disease resistance RPP13-like protein), AhRPS2 (AH02G06490, disease resistance protein RPS2), AhSGT1 (AH03G44120, SUPPRESSOR OF G2 ALLELE OF *skp1*), AhARF6 (AH03G48640, auxin response factor 6), AhARF9 (AH05G24680, auxin response factor 9), AhCYP707A4 (AH08G00660, abscisic acid 8'-hydroxylase 4), AhMAPK (AH17G02880, mitogen-activated protein kinase), AhSBT1.7 (AH11G11360, subtilisin-like protease SBT1.7).

Figure S10. Co-expression regulatory network of hub genes. (a) Regulatory network of the dark violet module. (b) Regulatory

network of navajowhite2 module. The hub gene is in the middle of each circle, surrounded by the genes it regulates. The network diagram was drawn in cytoscape (AH16G08890: Pectinacetyltransferase, AH17G23980: endoglucanase, AH10G20860: subtilisin-like protease SBT1.8, AH04G14810: glucan endo-1,3-beta-glucosidase, AH03G06730: transcription factor RF2b).

Figure S11. Conserved domains and 3D structure analysis of AhPMEs and AhPME4 localization. (a) Conserved domains and motif predictions of seven PME in peanut used for Y2H analysis. (b) Three-dimensional structure diagram of 7 PMEs, drawn using the SWISS-MODEL online tool. (c) A schematic vector for subcellular localization of AhPME4 in *N. benthamiana*. AhPME localized at cytoplasm and nucleus with GFP as the control referred to Figure S3. Bar = 25 μ m.

Figure S12. Schematic illustration of mutant and complement T3Es strain generation. (a) Schematic diagram of mutant strain generation. (b) Schematic diagram of complement strain generation. U represents upstream, and D represents downstream.

Table S1. Candidate genes that interact with RipAU in peanuts.

Table S2. Differentially expressed genes (DEGs) responsive to *Ralstonia solanacearum* in peanut at the four periods (M75 means Δ RipAU).

Table S3. KEGG pathway enrichment of DEGs.

Table S4. Differentially expressed genes (DEGs) related to phytohormone biosynthesis and signal transduction (M75 means Δ RipAU).

Table S5. Differentially expressed genes (DEGs) of the PME gene family.

Table S6. Clustering of genes in different modules and the functional annotations.

Table S7. Hub genes analysis. (a) Hub genes in different modules (Note: The orange darker part is AhSBT1.7 gene). (b) Hub genes in different modules (Note: The orange darker part is AhSBT1.7 gene).

Table S8. Differentially expressed genes (DEGs) of the subtilisin-like protease gene family.

Table S9. Specific primer sequences used for this research.

REFERENCES

- Angot, A., Peeters, N., Lechner, E., Vaillau, F., Baud, C., Gentzbittel, L. et al. (2006) *Ralstonia solanacearum* requires F-box-like domain-containing type III effectors to promote disease on several host plants. *Proceedings of the National Academy of Sciences of the United States of America*, **103**(39), 14620–14625.
- Ashburner, M., Ball, C.A., Blake, J.A., Botstein, D., Butler, H., Cherry, J.M. et al. (2000) Gene ontology: tool for the unification of biology. *Nature Genetics*, **25**(1), 25–29.
- Ausubel, F.M. (2005) Are innate immune signaling pathways in plants and animals conserved? *Nature Immunology*, **6**(10), 973–979.
- Bethke, G., Grundman, R.E., Sreekanta, S., Truman, W., Katagiri, F. & Glazebrook, J. (2014) Arabidopsis PECTIN METHYLESTERASEs contribute to immunity against *Pseudomonas syringae*. *Plant Physiology*, **164**(2), 1093–1107.
- Caiying, G., Saleem, T., Wensong, X., Tao, Z., Xun, H., Huasong, Z. et al. (2021) The role of effector RipQ for virulence in *Ralstonia solanacearum* GMI1000. *Acta Phytopathologica Sinica*, **52**(5), 801–812.
- Chen, K., Wang, L., Chen, H., Zhang, C., Wang, S., Chu, P. et al. (2021) Complete genome sequence analysis of the peanut pathogen *Ralstonia solanacearum* strain Rs-P.362200. *BMC Microbiology*, **21**(1), 118.
- Cheng, D., Zhou, D., Wang, Y., Wang, B., He, Q., Song, B. et al. (2021) *Ralstonia solanacearum* type III effector RipV2 encoding a novel E3 ubiquitin ligase (NEL) is required for full virulence by suppressing plant PAMP-triggered immunity. *Biochemical and Biophysical Research Communications*, **550**, 120–126.
- Cong, S., Li, J.Z., Xiong, Z.Z. & Wei, H.L. (2022) Diverse interactions of five core type III effectors from *Ralstonia solanacearum* with plants. *Journal of Genetics and Genomics*, **50**, 341–352.
- Deng, Y., Li, J.Q., Wu, S.F., Zhu, Y.P., Cai, Y.W. & He, F.C. (2006) Integrated nr database in protein annotation system and its localization. *Computer Engineering*, **32**(5), 71–72.
- Duan, X., Zhang, Z., Wang, J. & Zuo, K. (2016) Characterization of a novel cotton subtilase gene GbSBT1 in response to extracellular stimulations and its role in *Verticillium* resistance. *PLoS One*, **11**(4), e0153988.
- Fajing, C., Xin, T., Mengyu, H., Jiao, D., Yang, Y. et al. (2018) Research progress of subtilases in the interaction of plant and pathogen. *Molecular Plant Breeding*, **16**(10), 3146–3153.
- Felsenstein, J. (1985) Confidence limits on phylogenies: an approach using the bootstrap. *Evolution*, **39**, 783–791.
- Figueiredo, A., Monteiro, F. & Sebastiana, M. (2014) Subtilisin-like proteases in plant-pathogen recognition and immune priming: a perspective. *Frontiers in Plant Science*, **5**, 739.
- Fujiwara, S., Kawazoe, T., Ohnishi, K., Kitagawa, T., Popa, C., Valls, M. et al. (2016) RipAY, a plant pathogen effector protein, exhibits robust γ -glutamyl cyclotransferase activity when stimulated by eukaryotic thioredoxins. *Journal of Biological Chemistry*, **291**(13), 6813–6830.
- Grefen, C. & Blatt, M.R. (2012) A 2in1 cloning system enables ratiometric bimolecular fluorescence complementation (rBiFC). *BioTechniques*, **53**(5), 311–314.
- Huang, D., Mao, Y., Guo, G., Ni, D. & Chen, L. (2022) Genome-wide identification of PME gene family and expression of candidate genes associated with aluminum tolerance in tea plant (*Camellia sinensis*). *BMC Plant Biology*, **22**(1), 306.
- Jones, J.D.G. & Dangl, J.L. (2006) The plant immune system. *Nature*, **444**(7117), 323–329.
- Jordá, L., Coego, A., Conejero, V. & Vera, P. (1999) A genomic cluster containing four differentially regulated subtilisin-like processing protease genes is in tomato plants. *The Journal of Biological Chemistry*, **274**(4), 2360–2365.
- Kanehisa, M. (2004) The KEGG resource for deciphering the genome. *Nucleic Acids Research*, **32**(90001), 277–280.
- Kaur, G., Iyer, L.M., Subramanian, S. & Aravind, L. (2018) Evolutionary convergence and divergence in archaeal chromosomal proteins and chromo-like domains from bacteria and eukaryotes. *Scientific Reports*, **8**(1), 6196.
- Kumar, S. (1996) A stepwise algorithm for finding minimum evolution trees. *Molecular Biology and Evolution*, **13**(4), 584–593.
- Kumar, S., Stecher, G. & Tamura, K. (2016) MEGA7: molecular evolutionary genetics analysis version 7.0 for bigger datasets. *Molecular Biology and Evolution*, **33**, 1870–1874.
- Langfelder, P. & Horvath, S. (2008) WGCNA: an R package for weighted correlation network analysis. *BMC Bioinformatics*, **9**(1), 559.
- Langmead, B., Trapnell, C., Pop, M. & Salzberg, S.L. (2009) Ultrafast and memory-efficient alignment of short DNA sequences to the human genome. *Genome Biology*, **10**(3), R25.
- Liuti, C., Yan, X., Xiang, L., Lin, M. & Junxiong, S. (2014) Analysis of effector proteins of type III secretion system in FOY_4 strain of *Ralstonia solanacearum*. *Tobacco Science & Technology*, **9**, 68–72.
- Lohou, D., Turner, M., Lonjon, F., Cazalé, A.C., Peeters, N., Genin, S. et al. (2014) HpaP modulates type III effector secretion in *Ralstonia solanacearum* and harbours a substrate specificity switch domain essential for virulence. *Molecular Plant Pathology*, **15**(6), 601–614.
- Long, S., Cao, Y., Li, Y. & Kang, Z. (2009) Metabolism of reactive oxygen species in the process of hypersensitive response of wheat to stripe rust. *Journal of Northwest A&F University*, **37**(11), 125–130 + 137.
- Luo, H., Pandey, M.K., Khan, A.W., Wu, B., Guo, J., Ren, X. et al. (2019) Next-generation sequencing identified genomic region and diagnostic markers for resistance to bacterial wilt on chromosome B02 in peanut (*Arachis hypogaea* L.). *Plant Biotechnology Journal*, **17**(12), 2356–2369.
- Moon, H., Pandey, A., Yoon, H., Choi, S., Jeon, H., Prokhorchik, M. et al. (2021) Identification of RipAZ1 as an avirulence determinant of *Ralstonia solanacearum* in *Solanum americanum*. *Molecular Plant Pathology*, **22**(3), 317–333.
- Nakano, M. & Mukaiyama, T. (2018) *Ralstonia solanacearum* type III effector RipAL targets chloroplasts and induces jasmonic acid production to

- suppress salicylic acid-mediated defense responses in plants. *Plant and Cell Physiology*, **59**(12), 2576–2589.
- Nakano, M., Oda, K. & Mukaihara, T.** (2017) *Ralstonia solanacearum* novel E3 ubiquitin ligase (NEL) effectors RipAW and RipAR suppress pattern-triggered immunity in plants. *Microbiology*, **163**(7), 992–1002.
- Naruya, S. & Nei, M.** (1987) The neighbor-joining method: a new method for reconstructing phylogenetic trees. *Molecular Biology and Evolution*, **4**, 406–425.
- Nemes, K., Gellért, Á., Almási, A., Vági, P., Sárny, R., Kádár, K. et al.** (2017) Phosphorylation regulates the subcellular localization of cucumber mosaic virus 2b protein. *Scientific Reports*, **7**(1), 13444.
- Niu, Y., Fu, S., Chen, G., Wang, H., Wang, Y., Hu, J.X. et al.** (2021a) Different epitopes of *Ralstonia solanacearum* effector RipAW are recognized by two *Nicotiana* species and trigger immune responses. *Molecular Plant Pathology*, **23**, 188–203.
- Otegui, M.S., Steelheart, C., Ma, W., Ma, J., Kang, B.H., De Medina Hernandez, V.S. et al.** (2024) Vacuolar degradation of plant organelles. *The Plant Cell*, **36**(9), 3036–3056.
- Qiao, H., Shen, Z., Huang, S.S.C., Schmitz, R.J., Ulrich, M.A., Briggs, S.P. et al.** (2012) Processing and subcellular trafficking of ER-tethered EIN2 control response to ethylene gas. *Science*, **338**(6105), 390–393.
- Qin, Z.** (2011) Optimization of *Agrobacterium*-mediated K326 genetic transformation system. *Journal of Anhui Agri*, **39**(8), 4436–4437.
- Ramirez, V., López, A., Mauch-Mani, B., Gil, M.J. & Vera, P.** (2013) An extracellular subtilase switch for immune priming in *Arabidopsis*. *PLoS Pathogens*, **9**(6), e1003445.
- Rautengarten, C., Usadel, B., Neumetzler, L., Hartmann, J., Büssis, D. & Altmann, T.** (2008) A subtilisin-like serine protease essential for mucilage release from *Arabidopsis* seed coats. *The Plant Journal*, **54**(3), 466–480.
- Saez-Aguayo, S., Ralet, M.C., Berger, A., Botran, L., Ropartz, D., Marion-Poll, A. et al.** (2013) PECTIN METHYLESTERASE INHIBITOR6 promotes *Arabidopsis* mucilage release by limiting methylesterification of homogalacturonan in seed coat epidermal cells. *Plant Cell*, **25**(1), 308–323.
- Saito, R., Smoot, M.E., Ono, K., Ruschinski, J., Wang, P.L., Lotia, S. et al.** (2012) A travel guide to cytoscape plugins. *Nature Methods*, **9**(11), 1069–1076.
- Sasaki, N., Takashima, E. & Nyunoya, H.** (2018) Altered subcellular localization of a tobacco membrane raft-associated remorin protein by tobamovirus infection and transient expression of viral replication and movement proteins. *Frontiers in Plant Science*, **15**(9), 619.
- Serrano, I., Buscaill, P., Audran, C., Pouzet, C., Jauneau, A. & Rivas, S.** (2016) A non canonical subtilase attenuates the transcriptional activation of defence responses in *Arabidopsis thaliana*. *eLife*, **5**, 5.
- Silva-Sanzana, C., Celiz-Balboa, J., Garzo, E., Marcus, S.E., Parra-Rojas, J.P., Rojas, B. et al.** (2019) Pectin methylesterases modulate plant homogalacturonan status in defenses against the aphid *Myzus persicae*. *Plant Cell*, **31**(8), 1913–1929.
- Sun, Y., Li, P., Shen, D., Wei, Q., He, J. & Lu, Y.** (2019) The *Ralstonia solanacearum* effector RipN suppresses plant PAMP-triggered immunity, localizes to the endoplasmic reticulum and nucleus, and alters the NADH/NAD⁺ ratio in *Arabidopsis*. *Molecular Plant Pathology*, **20**(4), 533–546.
- T UniProt Consortium.** (2018) Corrigendum UniProt: the universal protein knowledgebase. *Nucleic Acids Research*, **45**, 158–169.
- Tan, X., Qiu, H., Li, F., Cheng, D., Zheng, X., Wang, B. et al.** (2019) Complete genome sequence of Sequevar 14M *Ralstonia solanacearum* strain HA4-1 reveals novel type III effectors acquired through horizontal gene transfer. *Frontiers in Microbiology*, **10**, 1893.
- Tatusov, R.L., Galperin, M.Y., Natale, D.A. & Koonin, E.V.** (2000) The COG database: a tool for genome-scale analysis of protein functions and evolution. *Nucleic Acids Research*, **28**(1), 33–36.
- Tornero, P., Conejero, V. & Vera, P.** (1997) Identification of a new pathogen-induced member of the subtilisin-like processing protease family from plants. *The Journal of Biological Chemistry*, **272**(22), 14412–14419.
- Untergasser, A., Cutcutache, I., Koressaar, T., Ye, J., Faircloth, B.C., Remm, M. et al.** (2012) Primer3—new capabilities and interfaces. *Nucleic Acids Research*, **40**(15), e115.
- Wang, S., Meng, K., Luo, H., Yao, B. & Tu, T.** (2020) Research progress in structure and function of pectin methylesterase. *Chinese Journal of Biotechnology*, **36**(6), 1021–1030.
- Wang, Y., Zhao, A., Morcillo, R.J.L., Yu, G., Xue, H., Rufian, J.S. et al.** (2021) A bacterial effector protein uncovers a plant metabolic pathway involved in tolerance to bacterial wilt disease. *Molecular Plant*, **14**(8), 1281–1296.
- Weis, B.L., Kovacevic, J., Missbach, S. & Schleiff, E.** (2015) Plant-specific features of ribosome biogenesis. *Trends in Plant Science*, **20**(11), 729–740.
- Xia, X.** (2017) DAMBE6: new tools for microbial genomics, Phylogenetics, and molecular evolution. *Journal of Heredity*, **108**(4), 431–437.
- Xian, L., Yu, G., Wei, Y., Rufian, J.S., Li, Y., Zhuang, H. et al.** (2020) A bacterial effector protein hijacks plant metabolism to support pathogen nutrition. *Cell Host & Microbe*, **28**(4), 548–557.e7.
- Xu, Y. & Xu, Q.** (2018) Transformation of *Arabidopsis thaliana* by floral dip. *Bio-101*.
- Yu, G., Derkacheva, M., Rufian, J.S., Brillada, C., Kowarschik, K., Jiang, S. et al.** (2022) The *Arabidopsis* E3 ubiquitin ligase PUB4 regulates BIK1 and is targeted by a bacterial type-III effector. *The EMBO Journal*, **41**, e107257.
- Zhang, C., Chen, H., Cai, T., Deng, Y., Zhuang, R., Zhang, N. et al.** (2017) Overexpression of a novel peanut NBS-LRR gene AhRRS5 enhances disease resistance to *Ralstonia solanacearum* in tobacco. *Plant Biotechnology Journal*, **15**(1), 39–55.
- Zhang, C., Chen, H., Zhuang, R.R., Chen, Y.T., Deng, Y., Cai, T.C. et al.** (2019) Overexpression of the peanut CLAVATA1-like leucine-rich repeat receptor-like kinase AhRLK1 confers increased resistance to bacterial wilt in tobacco. *Journal of Experimental Botany*, **70**(19), 5407–5421.
- Zheng, X., Li, X., Wang, B., Cheng, D., Li, Y., Li, W. et al.** (2019) A systematic screen of conserved *Ralstonia solanacearum* effectors reveals the role of RipAB, a nuclear-localized effector that suppresses immune responses in potato. *Molecular Plant Pathology*, **20**(4), 547–561.